

Advances in Shape-Memory Polymers and Composites for Biomedical Device Applications

Chengjun Zeng, Liwu Liu, Wei Zhao, Xiaozhou Xin, Yanju Liu,* and Jinsong Leng*

Over the past two decades, remarkable advancements have been achieved in stimulus-responsive shape-memory polymers (SMPs), which exhibit desirable properties such as shape-memory characteristics, deformability, and biocompatibility, while responding to external stimuli. The development of shape-memory polymer composites (SMPCs) leads to high recovery forces and novel functionalities, including electrical actuation, magnetic actuation, and biocompatibility. The enhanced remotely controllable properties and functionality further expand the application of SMPs in biomedical areas, such as surgical applications for replacing handheld surgical instruments and drug delivery systems. In this review, the biomedical device applications of SMPs and SMPCs are focused on and their recent advancements in bone tissue scaffolds, lumen stents, and drug delivery carriers are examined. Furthermore, the bottlenecks and challenges encountered by SMPCs in biomedical devices are elucidated. The future development trend of SMPs and SMPCs is also discussed, aiming to provide valuable insights for broadening their applications in biomedical fields.

SMPs exhibit greater elasticity in their rubbery state compared to other shape-memory materials, including shape-memory alloys (SMAs) and shape-memory ceramics (SMCs). This characteristic endows SMPs with the capacity to achieve higher strain levels than SMAs and SMCs.^[10,11] Another advantage of SMPs is that their transition temperature can be adjusted according to the actual application requirements, which is achieved by tuning the concentration of the different component materials during the synthesis of SMPs.^[12–15] In manufacturing and engineering applications, the ability to customize the thermodynamic properties of materials to specific needs is important. By changing the chemical composition, SMPs can be tailored into biostructural materials that are biocompatible and biodegradable, which makes SMPs extremely promising for biomedical applications.^[16,17]

1. Introduction


In recent years, shape-memory polymers (SMPs) and shape-memory polymer composites (SMPCs) have attracted more and more attention in the biomedical field due to their special applications in the medical, electronic, and high-tech industries, as well as in daily life.^[1–4] SMPs are a class of stimulus-responsive polymers that are fixed into a temporary configuration by applying a certain external force to them in the heated state and then transformed from the temporary configuration to the original configuration by external environmental stimuli (e.g., heat, water, pH, electricity, magnetic field, humidity, etc.), the most common of which is thermal stimuli.^[5–9]

SMPC is a smart composite obtained by doping micro- and nanoparticles or fiber fillers into the SMP matrix, which substantially improves the mechanical properties of SMP without weakening the overall shape-memory properties and increases the actuation method.^[18–20] According to the different actuation mechanisms, SMPC can be classified into thermotropic,^[21,22] electro-tropic,^[23,24] phototropic,^[25,26] magnetostrophic,^[27,28] and chemically induced SMPC. Among these, thermotropic SMPCs have emerged as the primary choice for biomedical applications due to their easily controllable actuation methods, adjustable actuation temperatures, and minimal impact on human tissues.^[29,30] However, regulating the actuation temperature as well as the recovery rate of thermotropic SMPC to adapt to the human body has been an urgent problem. Electrotropic and magnetostrophic SMPCs are indirect thermotropic SMPCs, in which the temperature of the SMPC is increased under the action of an electric current or a magnetic field, and when the temperature reaches a critical state, the material starts to undergo shape recovery.^[31,32]

High-performance SMPs and SMPCs are attracting a lot of attention as smart materials in the field of clinical medicine and medical applications such as implantable medical devices.^[33–35] Extensive studies have explored the potential use of SMPs and SMPCs in minimally invasive procedures. These composites can expand from a compact state to their original shape upon external stimulation.^[36,37] Furthermore, SMP and SMPC medical devices exhibiting shape recovery activation generate a

C. Zeng, L. Liu, W. Zhao, X. Xin, Y. Liu
Department of Astronautical Science and Mechanics
Harbin Institute of Technology (HIT)
Harbin 150001, Heilongjiang, China
E-mail: yj_liu@hit.edu.cn

J. Leng
Center for Composite Materials and Structures
Harbin Institute of Technology (HIT)
Harbin 150080, Heilongjiang, China
E-mail: lengjs@hit.edu.cn

 The ORCID identification number(s) for the author(s) of this article can be found under <https://doi.org/10.1002/adem.202402145>.

DOI: 10.1002/adem.202402145

recovery force, demonstrating exceptional self-adaptation properties in various medical applications. Upon activation, these devices can conform precisely to complex anatomical structures, ensuring a snug fit and optimal performance even in challenging environments. This adaptive capability is particularly valuable for minimally invasive procedures and personalized medical treatments.^[38] **Figure 1** summarizes the possible applications of SMPs and SMPCs in some biomedical devices.^[39–44]

In summary, SMPs and SMPCs exhibit great potential for biomedical device applications due to their favorable functionality and shape-memory characteristics. This review mainly introduces the types of commonly used biocompatible and biodegradable SMPs, as well as the classification of bio-based SMPCs derived from these SMPs. It also summarizes the applications of bio-based SMPs and SMPCs in the field of biomedical devices, such as bone tissue scaffolds, luminal stents, and drug delivery carriers. Furthermore, it analyzes the challenges and future development trends of SMPs and SMPCs in biomedical applications, providing valuable insights for advancing research and enhancing patient care in this domain.

2. SMPC

2.1. Biocompatible and Biodegradable SMPs

Currently, biocompatible and biodegradable SMPs with great potential in the biomedical field include poly(ϵ -caprolactone) (PCL), polyurethane (PU), poly(lactic acid) (PLA), and poly(lactic-co-glycolic acid) (PLGA). PCL is a synthetic aliphatic polyester obtained through the ring-opening polymerization of ϵ -caprolactone.^[45] Under physiological conditions, PCL is gradually hydrolyzed to low-molecular-weight fragments, which are ultimately excreted through the body's metabolic pathways, exhibiting excellent biocompatibility.^[46] The degradation of PCL is relatively slow, but can be controlled by adjusting factors such as molecular weight, crystallinity, and morphology. This controllability makes it an ideal material for long-term drug delivery systems. In addition, PCL is easy to process into various shapes and structures, achieving a good balance between mechanical properties, biodegradability, and biocompatibility. As a result, it is widely used in several tissue engineering applications, including bone tissue, cartilage, nerves, cardiovascular tissue, and skin.^[47,48]



Figure 1. Overview of SMPs and SMPCs in biomedical applications. Bone tissue scaffold. Reproduced with permission.^[39] Copyright 2021, Elsevier. Tracheal stents. Reproduced with permission.^[40] Copyright 2022, Elsevier. Occlusion devices. Reproduced with permission.^[41] Copyright 2019, Wiley-VCH. Drug delivery devices. Reproduced with permission.^[42] Copyright 2023, Wiley-VCH. Bone screw. Reproduced with permission.^[43] Copyright 2020, Elsevier. Vascular stents. Reproduced with permission.^[44] Copyright 2019, Wiley-VCH.

Shape-memory PU (SMPU) is a smart polymer material with a unique molecular structure and excellent properties. Its typical structure consists of soft segments (usually polyester or polyether chains) and hard segments (urethane bonds).^[49] The urethane bonds in the molecular structure are biologically inert and therefore have good biocompatibility with human tissue and the physiological environment. By adjusting the ratio and chemical composition of the soft and hard segments, the material can be biodegradable, which is promising for biomedical applications.^[50] SMPU not only has excellent shape-memory properties and can accurately recover a preset shape under a specific temperature stimulus but also its biocompatibility and degradability bring great potential in the fields of tissue engineering, drug delivery, and implantable medical devices.

PLA is an aliphatic polyester derived from renewable resources. It is synthesized by polycondensation reaction of lactic acid monomers and has good biocompatibility and biodegradability. Its molecular structure consists of repeating lactate units, which can be divided into L-lactic acid and D-lactic acid stereoisomers.^[51,52] Different ratios of these isomers allow for the regulation of its physical and mechanical properties. The chemical structure of PLA features carbonyl and ester bonds, which endow it with outstanding biodegradability.^[53] In human tissues, PLA can be enzymatically hydrolyzed and metabolized, and ultimately converted to carbon dioxide and water, and therefore does not pose any environmental hazard. Thanks to its excellent biocompatibility, PLA shows broad application prospects in the fields of biomedicine and tissue engineering and packaging materials and has become the focus of sustainable materials research.^[54,55]

2.2. Classification and Actuation Methods of SMPCs

Based on biocompatible and biodegradable SMPs, SMPCs exhibit excellent mechanical properties, flexible actuation modes, and biocompatibility and therefore have a promising future in biomedical applications. SMPCs are mainly classified into three types: fiber-reinforced SMPCs,^[56] nanoparticle-reinforced SMPCs,^[57] and multipolymer-blended SMPCs.^[58] Fiber

reinforcement can increase the strength and modulus of SMPCs. Nanoparticle reinforcement enhances the thermal, electrical, and magnetic actuation properties of SMPCs. Blending multiple polymers broadens the actuation temperature range. **Table 1** summarizes the fabrication methods, actuation modes, and recovery forces of common bio-based SMPCs.

2.2.1. Fiber-Reinforced SMPCs

Fiber-reinforced SMPCs are a novel class of smart materials that have garnered significant attention in the biomedical field in recent years. SMPCs based on biocompatible and biodegradable polymers such as PCL, SMPU, and PLA exhibit immense potential in applications like tissue engineering scaffolds, biodegradable implants, and intelligent drug delivery systems.^[59] These SMPCs typically employ external stimuli such as heat, light, or electricity as activation methods, with thermal activation being the most commonly used due to its simplicity and controllability.

Research indicates that fiber reinforcement can markedly improve the mechanical properties, shape-memory effect, and biocompatibility of SMPCs. Carbon fibers, with their superior mechanical properties and electrical conductivity, are frequently used to enhance mechanical performance and enable electrical stimulus responsiveness.^[60] Biological fibers, such as cellulose and silk fibroin fibers, are highly regarded in tissue engineering scaffolds for their excellent biocompatibility and degradability. Kevlar fibers offer unique advantages in medical devices that require high strength and lightweight characteristics.^[61] The type, content, orientation, and distribution of fibers significantly influence the performance of SMPCs.^[21] Adequately increasing fiber content can enhance the material's recovery force and shape fixity ratio. However, excessive fiber content may result in a decline in shape recovery ratio. Fiber orientation has a considerable impact on the anisotropic behavior of SMPCs, and regulating fiber alignment can achieve directional deformation, which is particularly crucial in designing medical devices with specific functions.

The application of 3D-printing technology provides new avenues for the precise fabrication and complex structural design of

Table 1. Comparison of the compositions, fabrication methods, actuation modes, and recovery forces of common bio-based SMPCs.

Matrix	Reinforcement	Manufacturing method	Actuation method	Driving force			Reference
				High	Medium	Low	
PLA	Carbon fiber	4D printing	Electricity	•	–	–	[60]
PLA	Aramid fiber	4D printing	Thermal	•	–	–	[61]
PLA	Carbon fiber	4D printing	Thermal	•	–	–	[21]
SMPU	Black-phosphorus sheets	Solution casting	Photo	–	–	•	[63]
PCL	Fe ₃ O ₄ /CNTs	Injection	Magnetism	–	•	–	[64]
SMPU	Carbon nanotube (CNT)	Wet spinning	Electricity/thermal	•	–	–	[65]
PCL	Fe ₃ O ₄	3D printing	Magnetism	–	•	–	[67]
SMPU	Al ₂ O ₃	Physical blending	Thermal	–	–	•	[68]
PLA/ Polyethylene glycol blend	<i>Chamelea gallina</i> shells	Physical blending	Thermal	–	–	•	[71]
PLA/ poly (butylene adipate-co-terephthalate) blend	PVAc-grafted CNCs	3D printing	Thermal	–	•	–	[45]
PLA	Polyethylene glycol	4D printing	Thermal	–	•	–	[33]

SMPCs, making the preparation of customized medical implants and tissue engineering scaffolds feasible.^[62] The 4D printing further extends the intelligent deformation capabilities of SMPCs, offering new approaches for developing adaptive medical devices and intelligent drug delivery systems.^[5] For example, SMPC scaffolds fabricated using 4D printing can undergo predetermined shape changes when stimulated by body temperature, thereby better adapting to human tissue structures.

2.2.2. Nanoparticle-Reinforced SMPCs

Nanoparticle-reinforced SMPCs have demonstrated significant potential in biomedical applications. By using biocompatible and biodegradable SMPs as the matrix and introducing nanoparticles, the shape-memory performance and mechanical properties of the materials can be markedly improved.^[63] The addition of nanoparticles introduces multiple stimulus-responsive modes to SMPCs.^[64] For instance, incorporating conductive nanoparticles such as carbon nanotubes (CNTs) or graphene enables the material to respond to electrical stimuli, achieving electrically induced shape-memory effects.^[65] Introducing metallic or oxide nanoparticles imparts sensitivity to light or magnetic fields.^[66] For example, PCL-based SMPCs doped with magnetic nanoparticles can achieve contactless activation under an alternating magnetic field, making them suitable for remote control of in vivo implanted devices.^[67] Nanoparticle reinforcement also significantly enhances the recovery force of SMPCs. The high specific surface area of nanoparticles and their strong interfacial interactions with the matrix increase the modulus and strength of the composites.^[68] During the shape recovery process, a higher modulus contributes to a greater driving force, ensuring that the material reliably returns to its initial shape in complex environments. This is crucial for biomedical devices requiring precise shape recovery and substantial driving force, such as deployable implantable stents and minimally invasive surgical instruments.

In terms of fabrication, 3D/4D-printing technology utilizing nanoparticle-reinforced SMPCs has attracted widespread attention. By uniformly dispersing nanoparticles within a biodegradable polymer matrix, personalized medical devices with complex structures and functional gradients can be fabricated.^[69] In the biomedical field, nanoparticle-reinforced SMPCs are used to develop smart implants, biodegradable drug delivery systems, and tissue engineering scaffolds. For example, degradable bone tissue scaffolds prepared from PLA, upon the addition of nanoparticles, exhibit improved mechanical strength and photo responsiveness, promoting shape adjustment, and functional recovery during bone tissue regeneration.^[70]

2.2.3. Multipolymer-Blended SMPCs

Multipolymer-blended SMPCs are materials formed by blending two or more polymers, exhibiting shape-memory effects.^[71] These composites leverage the physical and chemical properties of different polymers to achieve precise control over the thermodynamic and mechanical properties of the material. As a result, they can return from a temporary shape to their original shape under external stimuli. Compared to single-component SMPs,

multipolymer-blended SMPCs offer significant advantages in tunability and functional diversity. Specific shape-memory properties can be attained by adjusting the types and ratios of the polymers used.

In recent years, biocompatible and biodegradable multipolymer-blended SMPCs have attracted widespread attention in the biomedical field.^[72] These materials typically utilize biodegradable polymers such as PLA and PCL to create composites that combine excellent shape-memory properties with desirable biological characteristics.^[45] The primary mode of actuation is thermal stimulation, employing the material's glass transition temperature (T_g) or melting temperature (T_m) to trigger shape recovery through body heat or external heating.^[33] Recovery force can be optimized by adjusting the molecular weight, crystallinity, and blending ratios of the polymers to meet the mechanical performance requirements of various biomedical devices. In terms of applications, these materials have been explored for use in degradable stents and controlled drug release systems, demonstrating the potential to promote tissue regeneration, reduce surgical invasiveness, and enhance patient comfort.

3. Application in Bone Tissue Scaffolds

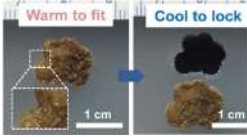

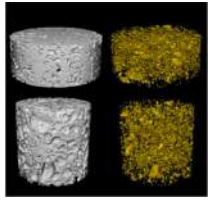
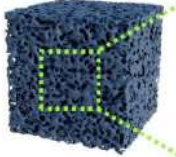

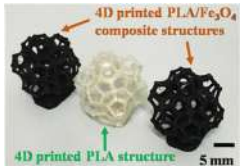
SMPs and SMPCs are potential candidates for reconfigurable scaffolds for the treatment of irregular bone defects because SMP- and SMPC-based scaffolds may be extruded into irregular bone defects above their transition temperature.^[16,73–75] Polymers such as PCL,^[76] SMPU,^[77] and PLA^[78] possess shape-memory properties activated by heat, and their unique shape-memory properties can simplify some complex grafting procedures in clinical applications.^[79,80] In addition, excellent chemical stability, good biocompatibility and biodegradability make them more widely used in bone tissue engineering.^[81] **Table 2** summarizes the application of different SMPCs in bone tissue scaffolds and the comparison of their performance.

3.1. PCL-Based Composite Scaffolds

Developing bioelectrically active SMPs with tunable transition temperatures for tissue engineering remains challenging.^[82,83] Deng et al.^[84] developed electrically active stretchable shape-memory copolymers using PCLs of different molecular weights and conductive aniline trimers (ATs) and confirmed their advantages in enhancing the differentiation of myoblasts (C2C12). The results of shape recovery experiments are shown in **Figure 2a**, where PCL-AT copolymers with different molecular weights were able to return to their initial shape within 15 s. These SMPs with electrical activity, highly stretchable, biodegradable, and glass transition temperatures near body temperature demonstrate significant advantages for bone tissue engineering applications.

Tissue engineering is currently the most effective treatment for critical-size craniomaxillofacial bone defects.^[85–87] PCL porous scaffolds with irregular boundary matching, interconnected porous networks, and good bioactivity of bone defects meet the ideal needs to promote bone tissue regeneration.^[88–90] Zhang et al.^[91] photo-cross-linked PCL diacrylate to prepare a shape-memory PCL porous scaffold. Applying a bioactive polymer coating to the pore walls enhanced the scaffolds' bioactivity,

Table 2. Comparison of the performance of bone tissue scaffolds based on different SMPCs.

Materials	Scaffold	Actuation method	Characteristics	Reference
Polydopamine-coated PCL		Thermal	Superior bioactivity and osteoblast adhesion	Reproduced with permission. ^[91] Copyright 2014, Elsevier.
PCL/hydroxyapatite nanocomposite		Thermal	Good cytocompatibility	Reproduced with permission. ^[92] Copyright 2014, American Chemical Society.
Polyethylene glycol and PCL		Thermal	Closely packed pore walls and reduced porosity	Reproduced with permission. ^[94] Copyright 2022, Elsevier.
SMPU and magnesium		Photo	Shape fixity ratio of 93.6% and shape recovery ratio of 95.4%	Reproduced with permission. ^[102] Copyright 2022, Elsevier.
Polytetrahydrofuran-based polyurethane		Thermal	Excellent biocompatibility and cell osteoconductive capacity	Reproduced with permission. ^[106] Copyright 2023, Elsevier.
PLA/hydroxyapatite		Thermal	Shape recovery of 98%	Reproduced with permission. ^[111] Copyright 2016, Elsevier.
PLA/Fe ₃ O ₄ composites		Magnetism	Biological activity and osteogenic effect	Reproduced with permission. ^[39] Copyright 2021, Elsevier.
PLA/Fe ₃ O ₄ composites		Thermal / magnetism	Physiologically relevant operating temperature range	Reproduced with permission. ^[117] Copyright 2019, Elsevier.

significantly improving osteoblast adhesion, proliferation, and the expression of osteogenesis-related genes. As shown in Figure 2b, in shape-memory experiments, the scaffolds softened when the external temperature exceeded the melting temperature (T_m) of PCL. An external force was then applied to form

a temporary shape corresponding to irregular defects. Upon cooling, the scaffold solidified in this temporary shape, allowing for precise defect filling.

Liu et al.^[92] recently developed a shape-memory nanocomposite scaffold loaded with bone morphogenetic protein 2 (BMP-2),

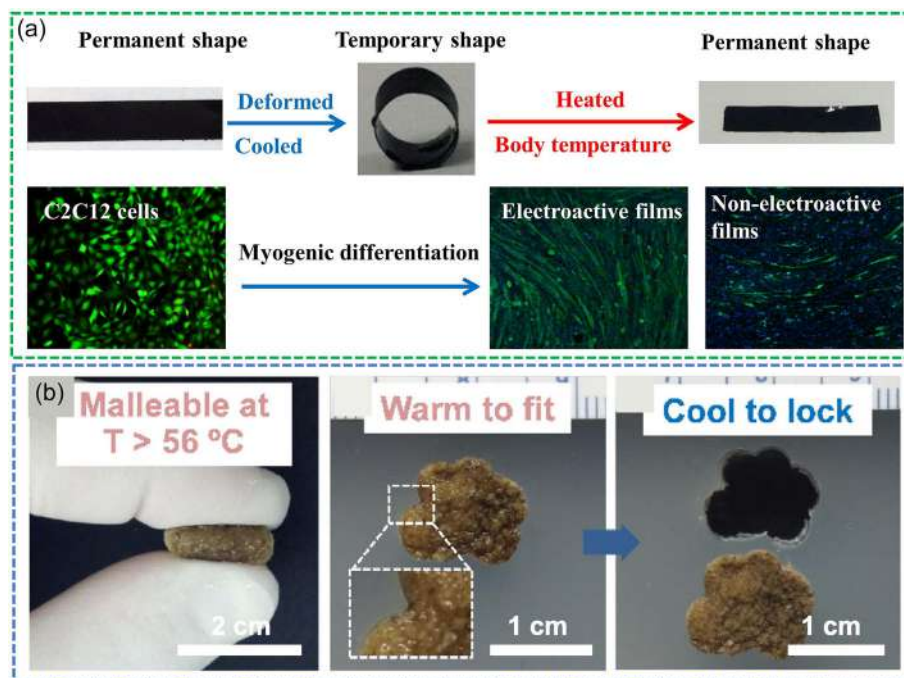


Figure 2. a) Shape-memory process of PCL-AT copolymer film. Reproduced with permission.^[84] Copyright 2016, Elsevier. b) Functional demonstration of polydopamine-coated PCL scaffolds. Reproduced with permission.^[91] Copyright 2014, Elsevier.

consisting of chemically cross-linked PCL (c-PCL) and hydroxyapatite (HAP) nanoparticles. The HAP nanoparticles enhanced the scaffolds' mechanical stability, osteoconductivity,^[93] and in vivo micro-CT image quality. In vitro shape-memory tests demonstrated complete recovery from the temporary to the original shape at 37 °C. The in vivo shape-memory recovery process of BMP-loaded nano-SMPC scaffolds was examined using a temperature pump at 42 °C during implantation to maintain the animals' temperature under anesthesia (Figure 3a). The 3D micro-CT images and quantitative analysis revealed increased bone formation in the SMPC scaffold group compared to the control group. SMPC scaffolds show promise in addressing large-volume scaffold implantation in complex and dynamic in vivo environments. This study offers a simple engineering approach for multifunctional scaffold implantation aimed at treating or repairing diseased human organs and tissues.

Wang et al.^[94] developed porous bone scaffolds utilizing a combination of hydrophilic poly(ethylene glycol), biodegradable PCL, and calcium citrate/amorphous calcium-phosphate-hybridized particles. The scaffolds were fabricated through a series of techniques, including bubbling, salt immersion, and freeze-drying. The resulting bone scaffolds demonstrated adjustable mechanical properties and pore structure, as well as remarkable shape-memory characteristics during thermal cycling. Figure 3b presents a morphological comparison of the porous bone scaffolds following compression recovery. The scanning electron microscope images reveal that the compressed sample exhibits extruded pores with closely packed pore walls and reduced porosity. However, upon heating, the scaffold regains its original shape, and the morphology and structure of the pores are restored, as evidenced by micro-CT reconstruction images of

the pore structure. The scaffold's ability to adopt a less traumatic temporary shape at elevated temperatures and revert to its permanent shape upon reheating offers significant advantages. This feature allows for minimally invasive implantation procedures, reduces the risk of surgical infections, and enables rapid transformation within the body fluid environment.

3.2. SMPU-Based Composite Scaffolds

In recent studies, Yu et al.^[95] synthesized novel SMPUs using a combination of diphenylmethane 4,4'-diisocyanate, adipic acid, ethylene glycol, ethylene oxide, poly(propylene oxide), and 1,4-butanediol. They employed the salt particle leaching method to create SMPU porous scaffolds with adjustable pore sizes by varying the size of the salt particles. These scaffolds exhibit excellent mechanical properties suitable for bone repair, tunable pore size, and remarkable shape-memory characteristics. Moreover, they possess the ability to promote cell proliferation, making them promising candidates for bone tissue engineering applications. Shuai et al.^[96] fabricated SMPU scaffolds doped with multi-walled CNTs (MWCNTs) utilizing selective laser sintering. The scaffolds containing 1.5 wt% MWCNTs exhibited a shape fixity rate of 95.6% and a shape recovery rate of 90.2%. Cell culture studies demonstrated that these scaffolds possess commendable cell compatibility, which promotes cell adherence and proliferation. MWCNTs were further subjected to convective self-assembly on a tetrapodal ZnO (t-ZnO) template, after which the resultant t-ZnO@MWCNT assemblies were embedded within SMPU scaffolds to endow them with electro-induced shape-memory properties.^[97] Under the combined influence

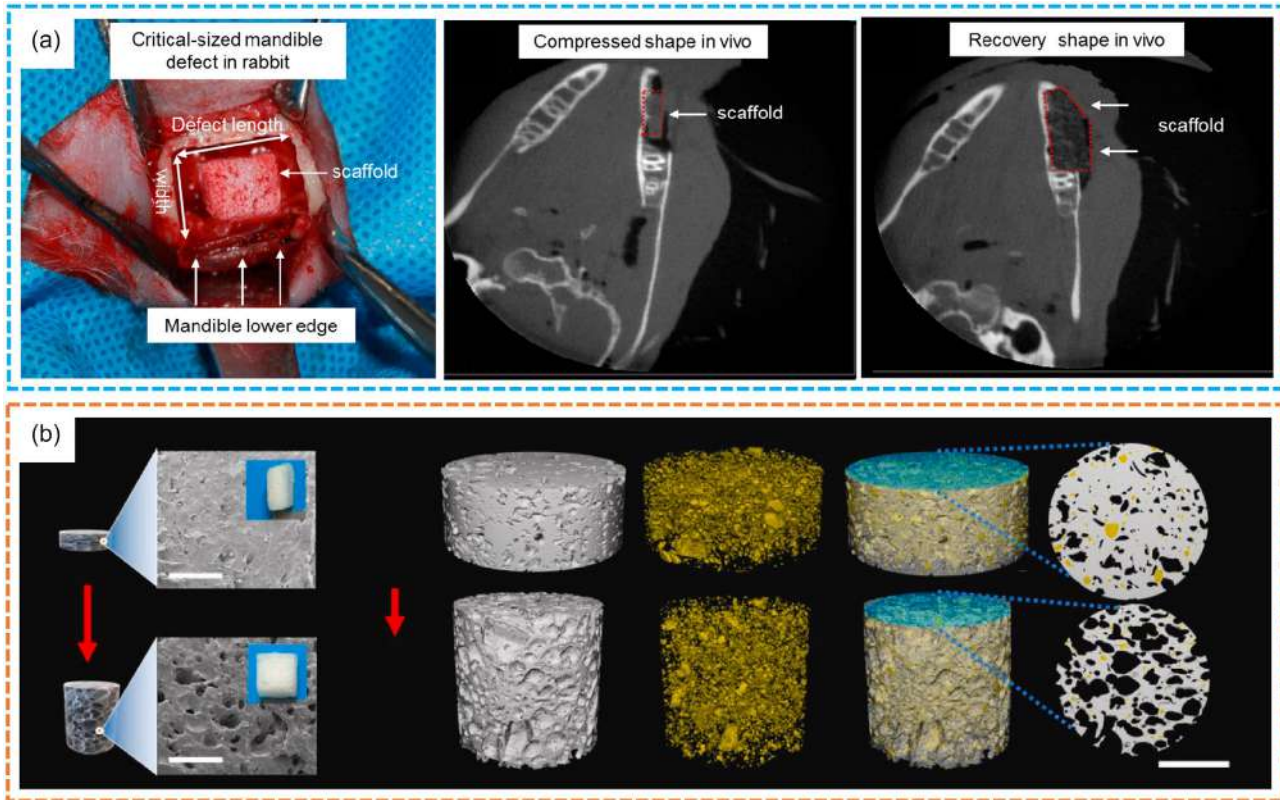


Figure 3. a) In vivo shape-memory recovery process of BMP-2-loaded SMPC scaffolds observed by cone-beam-computed tomography. Reproduced with permission.^[92] Copyright 2014, American Chemical Society. b) Macroscopic and microscopic images of porous bone scaffolds before and after shape recovery. Reproduced with permission.^[94] Copyright 2022, Elsevier.

of t-ZnO and electrical stimulation, these scaffolds demonstrated enhanced osteogenic induction capabilities.

Numerous investigations have been undertaken in recent years to explore the adaptive behavior of SMPs, with the majority of these studies focusing on in vitro validation.^[98–100] Henderson et al.^[101] developed an acrylate-based SMP implant, which served as a synthetic bone substitute in a model of weight-bearing femoral segmental defects. Recently, a novel PU/HAP-based SMPC porous foam was fabricated using the gas foaming method for the treatment of weight-bearing bone defects.^[93] Previously, SMPU has been used to treat cerebral aneurysm embolism. Zhang et al.^[102] reported a NIR-responsive bone tissue scaffold, which was made of SMPU and magnesium (Mg) by 3D-printing technique. The fabricated scaffold could be heated to recovery within 60 s under NIR irradiation. With a magnesium content of 4 wt%, the scaffold exhibited a shape fixed rate of 93.6% and a shape recovery rate of 95.4%. **Figure 4a** shows the shape recovery process of this bone tissue scaffold and a schematic diagram of the scaffold being implanted into the skull and repairing the bone defect with the aid of near-infrared light.

Repairing articular cartilage defects poses a significant challenge in orthopedic surgery owing to its limited self-regenerative capacity.^[103,104] Deng et al.^[105] obtained an SMPC scaffold for cartilage defect repair by doping nano-HAP in SMPU matrix. After coculturing fibroblasts with the SMPC scaffold for 3 days, the cell survival rate was more than 95%, indicating that the

scaffold had good cytocompatibility. When the SMPC scaffold was implanted subcutaneously in rats, the tissue around the scaffold was covered by fibroblasts with neovascularization. In conclusion, the SMPC scaffold demonstrated excellent in vivo histocompatibility after implantation.

To meet the requirements of antimicrobial properties and biocompatibility, Luo et al.^[106] processed SMPU composite scaffolds for minimally invasive alveolar bone restorations by combining in situ polymerization and gas foaming methods. SMPU was doped with citrate-functionalized amorphous calcium phosphate as an antimicrobial factor to achieve outstanding antimicrobial properties of the composite scaffold. **Figure 4b** depicts the microstructures of the SMPU composite scaffolds before and after compression and bending deformation recovery. It was observed that no pore collapse occurred after compression deformation of the scaffolds, and the pore structure was restored to its initial state when the macroscopic shape returned to its original shape. Furthermore, in vitro experiments verified the excellent biocompatibility and cellular osteogenic potential of the composite scaffold.

3.3. PLA-Based Composite Scaffolds

PLA is a thermoplastic SMP that is widely used in 3D printing due to its high modulus of elasticity, relatively low glass

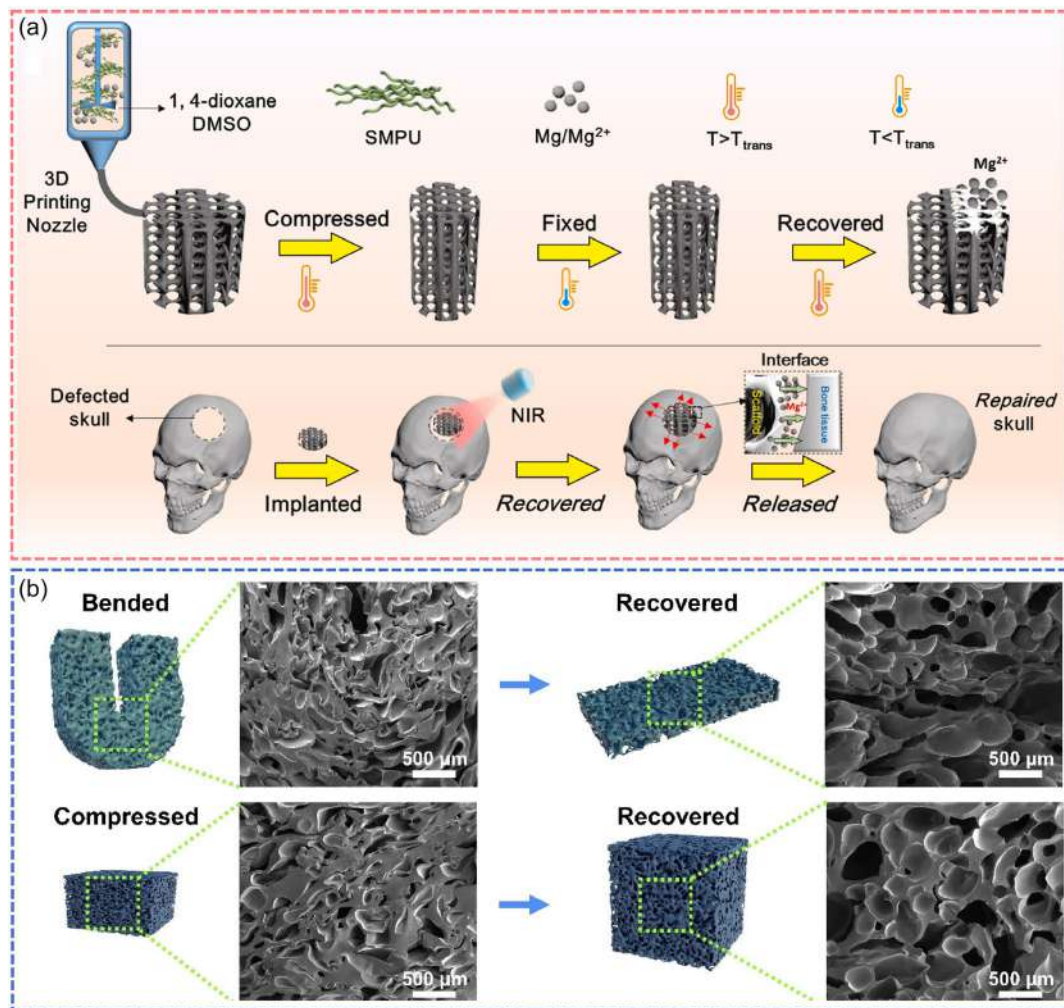


Figure 4. a) Schematic diagram of the shape recovery process of SMPU/Mg scaffold and bone defect repair. Reproduced with permission.^[102] Copyright 2022, Elsevier. b) Microstructure of SMPU composite scaffolds before and after compression and bending deformation recovery. Reproduced with permission.^[106] Copyright 2023, Elsevier.

transition temperature (55–65 °C), and excellent shape-memory properties.^[61,107] Long PLA chains can act as a stationary phase through physical entanglement, while the polymer chains between the entanglement can be stretched into temporary shapes during deformation.^[108] In recent years, shape-memory PLA has received increasing attention in medical applications.^[109,110]

Senatov et al.^[111] produced fusible filaments by combining PLA and 15 wt% HAP and then constructed PLA/HAP bone repair scaffolds with porous structures using a 3D printer. The scaffolds had an average pore size of $\approx 700 \mu\text{m}$ and a porosity of 30%, which could satisfy the structural requirements for bone marrow mesenchymal stem cells growth within the scaffolds. The inclusion of HAP reduced the heat conduction rate and increased the material's glass transition temperature from 53 to 57 °C. Shape-memory experiments showed that the PLA/HAP porous scaffolds could withstand three consecutive compression–heating–compression cycles without delamination (Figure 5a), and the shape recovery rate could reach 98%. During the heating process, the shape-memory effect will make

the bone repair scaffold gradually reduce the bone cracks, thus realizing self-repair, which provides a new direction for the use of autologous implants in the treatment of small bone defects.

Subsequently, an *in vitro* biological assessment of the 3D-printed PLA/HAP porous scaffolds was conducted.^[112] MSCs were tested for the presence of characteristic hematopoietic and endothelial markers by flow cytometry. Fibroblasts were observed to exhibit spindle morphology using light microscopy. Figure 5b shows that MSC cells were widely distributed and formed strong interactions with the scaffold surface. In addition, aggregated MSC cells are observed inside the channels of the scaffold as well as on the surface, indicating that the cells grow in a 3D manner. Normally, cells need to be firmly adhered to the surface of the matrix to spread, proliferate, and maintain cellular functions. Wang et al.^[113] used low-temperature 4D-printing technology to fabricate reconfigurable bone tissue scaffolds for the treatment of irregularly shaped bone defects. The thermo-responsive matrix and on-demand near-infrared irradiation

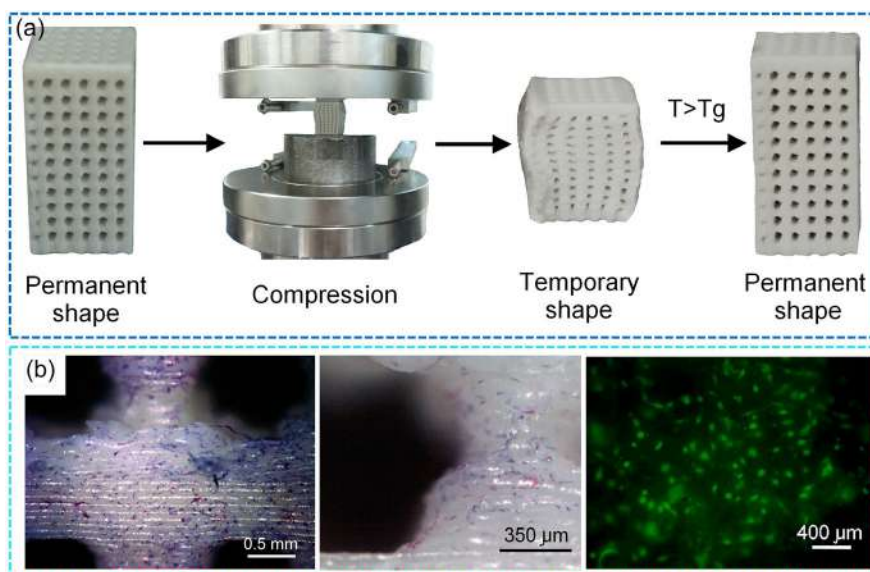


Figure 5. a) Demonstration of shape-memory effect of 3D-printed PLA/HAP scaffolds. Reproduced with permission.^[111] Copyright 2016, Elsevier. b) MSC cells on the surface of 3D-printed PLA/HAP porous scaffold. Reproduced with permission.^[112] Copyright 2017, Elsevier.

make the scaffolds easy to implant through a narrow channel in irregularly shaped bone defects.

There are a large number of porous structures in nature, which are of interest for the design of bone tissue scaffolds.^[114–116] Zhao et al.^[39] designed and prepared PLA/Fe₃O₄ porous bone tissue scaffolds mimicking lotus root and bone trabeculae, and elucidated the changes in their mechanical properties through theory and experiment. Due to the magneto-thermal effect of Fe₃O₄ particles, the PLA/Fe₃O₄ bone tissue scaffolds show satisfactory shape-memory effects under the effect of alternating magnetic fields. **Figure 6a** illustrates the shape recovery process of PLA/Fe₃O₄ bone tissue scaffolds under a 30 KHz magnetic field, from which it is observed that the scaffolds recovered to the initial shape within 15 s and the shape recovery rate was higher than 95.5%.

Zhang et al.^[117] prepared biocompatible PLA filaments reinforced with Fe₃O₄ particles, then processed bionic scaffolds with the shape of spinal bones using the magnetic Fe₃O₄/PLA composite filaments, and demonstrated their shape deployment process under an external magnetic field. The Fe₃O₄/PLA composite bionic scaffolds could revert to their initial shape within 100 s under the magnetic field, indicating that scaffolds with different sizes can be customized to fit bone defects as needed. **Figure 6b** shows the mechanism of the composite bionic scaffold as a bone repair tool. Here, it is envisioned that the bionic scaffold is first compressed to a smaller size and memorized to its original large size. It is then implanted into the bone defect site, where the compressed structure can be expanded to the desired shape under remote actuation by a magnetic field.

4. Application in Lumen Stents

There are multiple luminal organs or tissue structures in the human body, such as blood vessels,^[118] trachea,^[119,120] and

intestines.^[121] When these tissues become diseased or blocked, interventional therapy is often required, which is a painful process due to the large incisions required. SMP and SMPC stents facilitate implantation and therefore have great potential for use in the treatment of vascular, tracheal, and intestinal blockages.^[11,122] SMP and SMPC lumen stents are often required to have excellent mechanical properties and flexibility and to allow the geometric configuration to be adapted in the time dimension to accommodate lumen growth.^[123]

4.1. Vascular Stents

Currently, there are three main types of cardiovascular disease treatment: medication,^[124] bypass surgery,^[125] and vascular stent intervention.^[126] In contrast, medication is slow, while bypass surgery carries greater risks and can cause greater harm to the human body. Vascular stent intervention has obvious advantages, not only minimally invasive but also highly efficient, and currently plays an important role in the treatment of vascular stenosis.^[127,128] Vascular stents can support the blood vessels well and restore the normal function of the narrowed part of the blood vessels.^[129] Vascular stent intervention is a promising way to treat cardiovascular diseases.

At present, the commonly used materials for vascular stents mainly include 316L stainless steel, alloy materials^[130] and polymer materials.^[131] The nickel–titanium alloy and lead alloy are the more widely used alloy stent materials.^[132] Nitinol stents are easier to use and less damaging, making them more advantageous in clinical applications.^[133] **Figure 7a** illustrates a schematic diagram of the treatment of arterial stenosis using a crimped metal stent.^[134] A convoluted metal stent with a folded balloon attached is initially inserted via a medical catheter into the blocked blood vessel. The folded balloon is then inflated to expand the stent and push the plaque aside. However, this

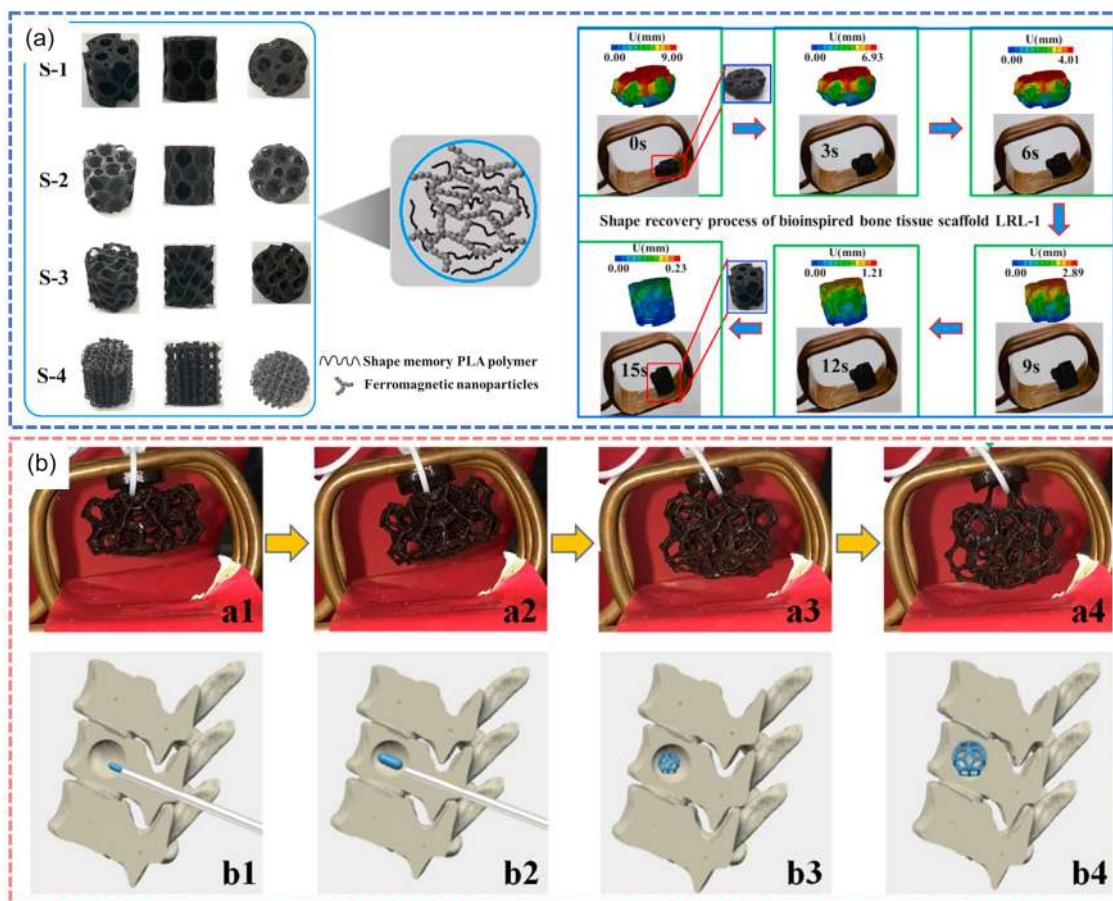


Figure 6. a) PLA/Fe₃O₄ composite bone tissue scaffold mimicking lotus root and its magnetically driven shape recovery process. Reproduced with permission.^[39] Copyright 2021, Elsevier. b) Mechanism of Fe₃O₄/PLA composite bionic scaffolds as a bone repair tool. Reproduced with permission.^[17] Copyright 2019, Elsevier.

balloon-expanded metal stent is not readily degraded by the intravascular environment, potentially causing mechanical damage to the vessel. Polymer stents are mainly made of SMPs or SMPs, which can be deformed in response to a variety of external stimuli, and the degradable properties as well as biocompatibility make them very promising for application. The polymer materials commonly used to prepare degradable vascular stents are mainly PLA and polyethylene. A schematic diagram of SMP vascular stent for minimally invasive surgery is given in Figure 7b.^[134] Prior to implantation, the SMP stent is programmed into a compact temporary configuration, and after implantation the stent is heated appropriately to self-inflate and support the vessel.

Jia et al.^[135] produced biodegradable self-expanding vascular stents using shape-memory PLA, which can be compressed into temporary shapes with finer diameters for implantation. The compressed shape-memory PLA stents possessed excellent shape fixity capability and could recover to their initial state upon thermal stimulation. Lin et al.^[136] fabricated personalized vascular stents with negative Poisson's ratio structures, and shape-memory PLA was used as the raw material to achieve the shape-memory properties of vascular stents. In vitro feasibility tests showed that this vascular stent was able to rapidly dilate

simulated stenotic vessels, which demonstrated a promising application in the treatment of vascular stenosis. Shi et al.^[137] developed a two-way shape-memory cellulose vascular stent using a single cellulose membrane fabricated through an eco-friendly approach. By modifying the thickness and cutting orientation of the various layers, two-way shape-memory cellulose stents with diverse structures, including ring, coil, and spiral, were easily produced (Figure 7c). In vitro studies demonstrated that the helical two-way shape-memory cellulose stents could be shape-adjusted and effectively maintained blood vessel dilation.

Poly(d,l-lactide-co-trimethylene carbonate) (PLMC) is a well-biocompatible SMP. Wan et al.^[44] prepared a composite ink based on PLMC and personalized 4D shape-change structures by direct ink writing. The 4D shape-changing structure exhibits rapid response shape-memory behavior near body temperature (40–45 °C). Figure 8a illustrates the shape recovery behavior of 2D planar structure and 3D stent, which is suitable as an implant in the treatment of common cardiovascular diseases such as arterial stenosis. Wei et al.^[138] synthesized an ultraviolet (UV)-cross-linked-PLA-based composite ink and utilized the composite ink to fabricate shape-memory vascular stents with fast remote control and magnetic guidance properties. In vitro experiments showed that the diameter of stenotic vessels caused by

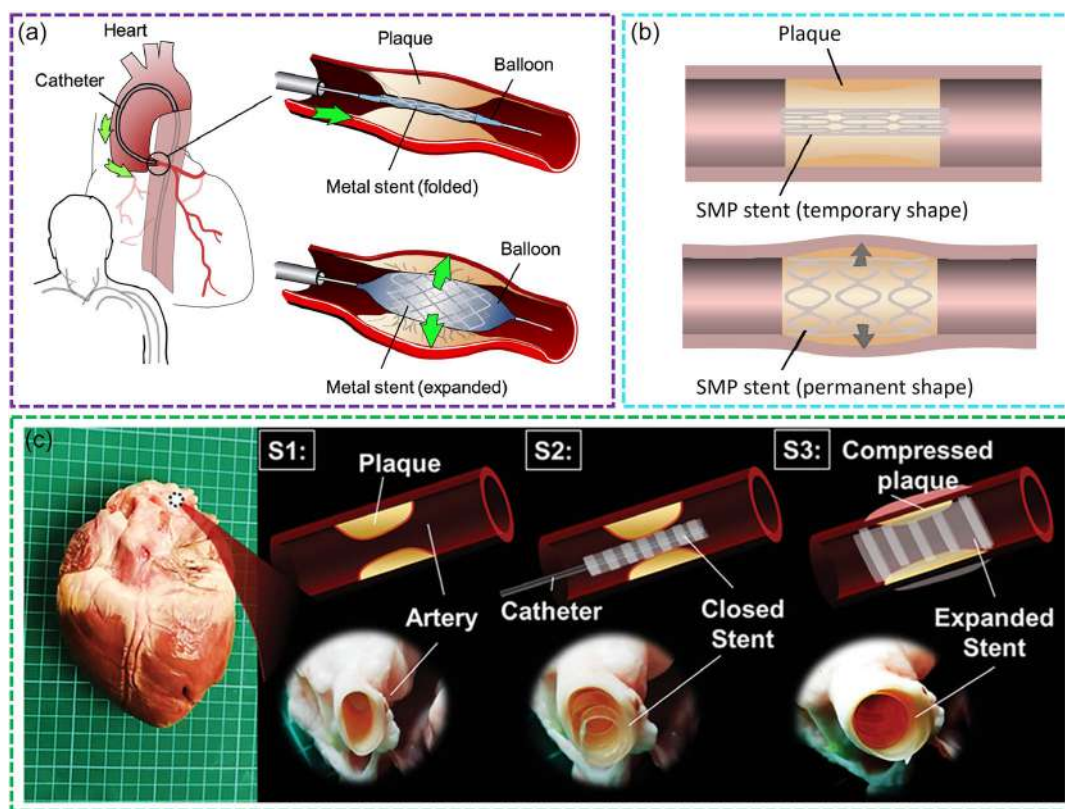


Figure 7. a) Schematic of the implantation of a balloon-expandable metal stent for arterial stenosis. Reproduced with permission.^[134] Copyright 2023, Elsevier. b) Schematic of deployment of SMP stent. Reproduced with permission.^[134] Copyright 2023, Elsevier. c) Vascular stents based on two-way shape-memory films. Reproduced with permission.^[137] Copyright 2021, Wiley-VCH.

thrombus could be re-expanded by applying the designed shape-memory vascular stents to maintain normal blood flow. This method provides greater design freedom for shape-memory vascular stents, which is important for the further development of user-defined vascular stents.

Zubir et al.^[139] fabricated a palm oil polyol (POP)-doped SMPU with shape fixity rate and elongation at break of 100 and 245%, respectively. POP-based SMPUs have desirable thermal properties as well as excellent shape-memory behavior, which makes them suitable as potential candidates for cardiovascular stents. Li et al.^[140] created a biodegradable magnetic shape-memory micro-anchor, composed of PLA impregnated with Fe₃O₄ nanoparticles, which demonstrates a thermally activated shape recovery mechanism within a temperature range suitable for human applications. Chen et al.^[141] manufactured a nanocomposite based on SMP and CNTs that enables electric actuation through uniform Joule heating of the self-heated CNT networks.

Vascular stents fabricated from this nanocomposite demonstrated stable support in the abdominal aorta of sheep. Zhang et al.^[142] employed a hot pressing and programming technique to fabricate a novel water-induced expandable bilayer vascular graft with an inner layer of cPCL and an outer layer of regenerated chitosan/polyvinyl alcohol (PVA) water-induced SMP (Figure 8b). This graft exhibited favorable mechanical properties, hemocompatibility, and both *in vitro* and *in vivo* biocompatibility.

Navigating catheters through complex vascular pathways, such as sharp turns or multiple U-shaped bends, remains a challenge for vascular embolization. Peng et al.^[143] proposed a novel multistage vascular embolization strategy for hard-to-reach vessels, which involves deploying unconstrained swimmable shape-memory magnetic microrobots (SMMs) from an existing catheter at the bifurcation point of the vessel. These SMMs are capable of agile movement in narrow and tortuous vessels, utilizing helical propulsion from rotating magnetic fields to navigate upstream. This multistage embolization technique was validated *in vivo* on rabbits, achieving navigation and renal artery embolization within 2 min over a distance of 100 centimeters. Liu et al.^[144] synthesized a durable immune-modulating nanofibrous niche (DINN) with exceptional processability, mechanical properties, and shape-memory functionality. Vascular stents based on the DINN demonstrated excellent therapeutic outcomes in *in vivo* trials.

4.2. Tracheal Stents

Tracheal stents are employed to alleviate tracheal obstruction.^[145] Currently, the primary types of tracheal stents include silicone stents,^[146] expandable metal stents,^[147] and biodegradable stents.^[148] While silicone stents are affordable and well-tolerated, they may migrate and deform, making them challenging to

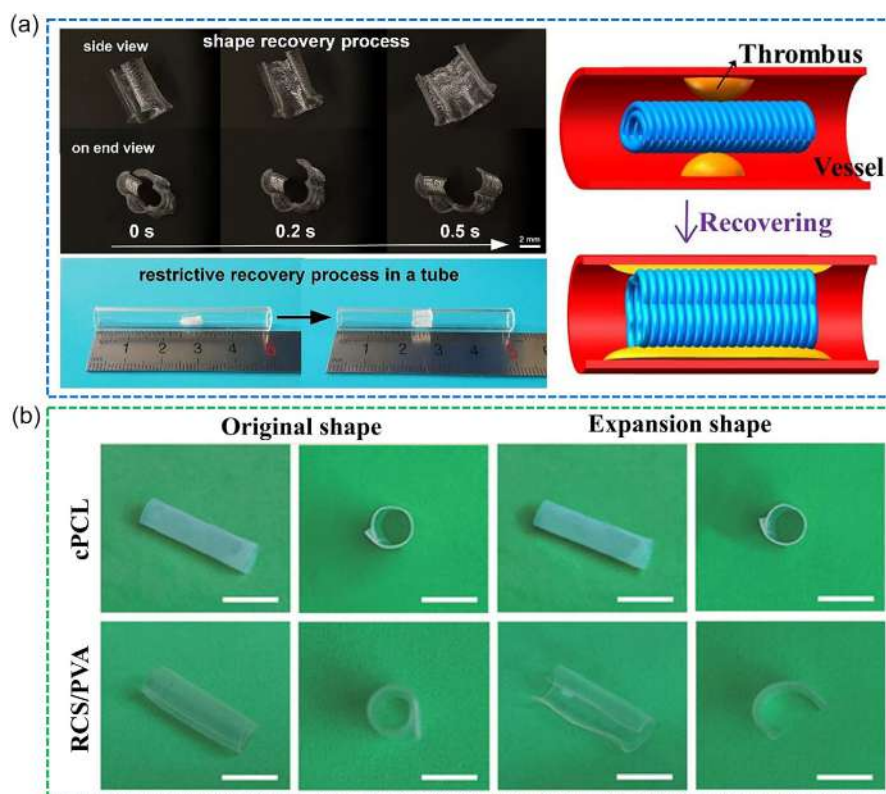


Figure 8. a) Schematic of the shape recovery process of the 4D-printed SMP structure and its use as a vascular stent. Reproduced with permission.^[44] Copyright 2019, Wiley-VCH. b) The original and expansion shapes of cPCL/RCP vascular grafts. Reproduced with permission.^[142] Copyright 2024, Wiley-VCH.

stabilize within the body. Expandable metal stents avoid mucus clogging. However, they are difficult to degrade and prone to complications. Biodegradable stents based on SMP and SMPC address the inherent limitations of silicone and metal stents, offering superior adaptation to the endotracheal environment and biodegradability, thereby presenting a novel therapeutic approach for trachea/bronchial obstruction diseases.^[149]

Zarek et al.^[150] prepared a PCL tracheal stent by UV light emitting diode stereolithography and performed a series of related tests. The findings indicated that a judicious choice of molecular weight could potentially modulate the transition temperatures of the materials, enabling the attainment of targeted shape fixity and shape recovery characteristics. Moreover, the stent adapts to the soft environment of the trachea and is structurally stable, which can effectively prevent tracheal blockage. Maity et al.^[151] described a shape-memory tracheal stent derived from a flexible photopolymerization ink, employing an in situ welding technique to achieve the connection between the thin and flexible layers. **Figure 9a,b** demonstrates the design scheme and flexibility of the shape-memory tracheal stent, respectively. The equilibrium between the stent's strength and flexibility can be attained by modifying the dimensions of the PCL blocks within the photopolymerization ink. The shape fixity and recovery rates of the ink surpassed 95 and 97%, respectively, suggesting outstanding shape-memory performance. **Figure 9c** depicts the shape recovery process of the tracheal stent, wherein the stent ultimately

restored its original shape following exposure to supraphysiological temperatures for 40 s.

Glass sponges possess a unique porous network architecture that can effectively meet the essential requirements of tracheal stents. This natural design offers excellent breathability and potential for tissue integration, making glass sponges an ideal bioinspired model for the development of next-generation tracheal stents. Inspired by the microstructure of glass sponges (**Figure 10a**), Zhao et al.^[152] designed an irregularly shaped tracheal stent and utilized shape-memory PLA/Fe₃O₄ composites for the production of tracheal scaffolds. **Figure 10b** gives 3D-sectional views of the bioinspired tracheal stent, which consists of a central skeleton and spiral ridges surrounding the wall. The designed bionic tracheal stent can be inserted into the human body in a temporary shape and restored to its intended shape through an alternating magnetic field. **Figure 10c** illustrates the shape recovery process of the bionic tracheal stent within the magnetic field, requiring 35 s, thus confirming successful in vitro functional verification. Compared with conventional tracheal stents, the shape-memory effects of the glass-sponge-inspired tracheal stent help to match the geometry of the trachea and are well suited for implantation in living organisms. Similarly, Zhang et al.^[122] fabricated an SMPC tracheal stent and achieved remote magnetic actuation by incorporating Fe₃O₄ particles into shape-memory PLA. The stent's shape recovery process required 40 s in an alternating magnetic field, resulting in a shape recovery rate exceeding 99%.

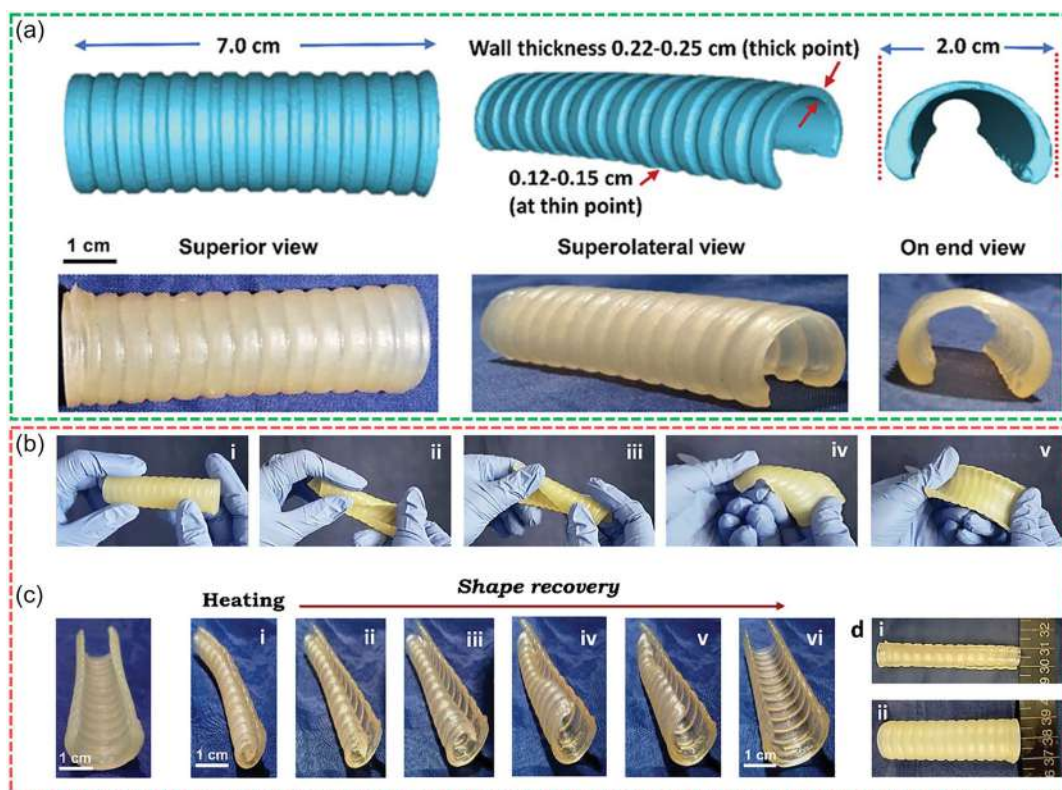


Figure 9. a) Designing and fabricating a shape-memory tracheal stent. b) Illustration depicting the stent's flexibility. c) Thermally induced shape recovery process of the tracheal stent. Reproduced with permission.^[151] Copyright 2021, Wiley-VCH.

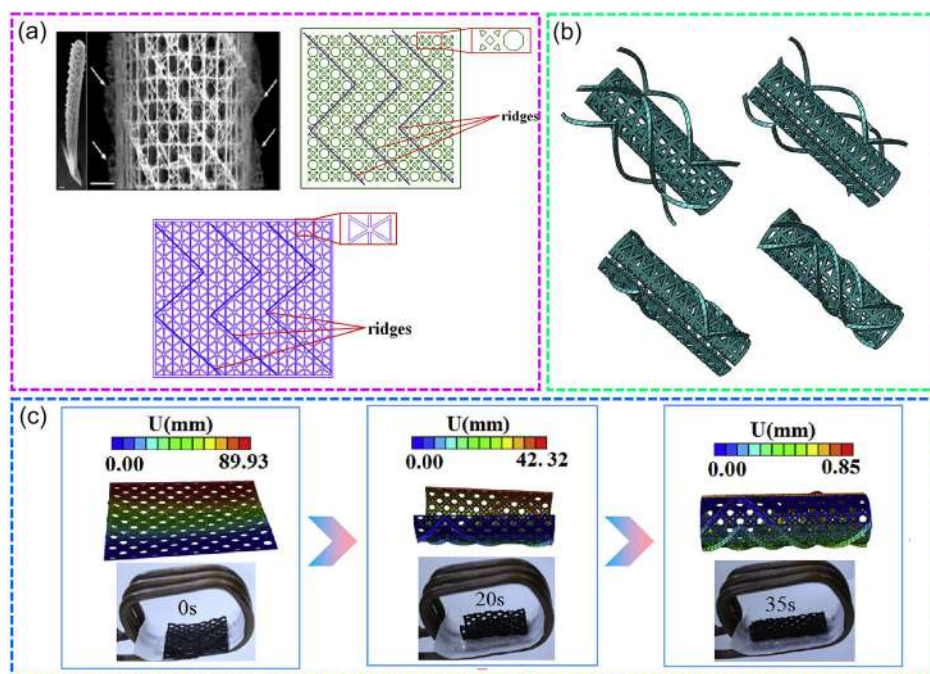


Figure 10. Glass-sponge-inspired SMPC tracheal scaffold. a) Schematic diagram of the overall skeleton and microstructure of the glass sponge. b) Design diagram of the glass-sponge-inspired tracheal scaffold. c) Shape recovery process of the bionic tracheal scaffold in a magnetic field. Reproduced with permission.^[152] Copyright 2019, Elsevier.

Zhao et al.^[40] recently fabricated shape-memory PCL/Fe₃O₄ composites, where the addition of magnetic nanoparticles imparted the capability for remote and noncontact actuation to the PCL/Fe₃O₄ composite. Based on the shape-memory PCL/Fe₃O₄ composite, a biomimetic SMPC tracheal stent was designed (Figure 11a). This SMPC tracheal stent was able to be spread out into a planar shape and then deformed into a 3D cylinder shape driven by a magnetic field (Figure 11b). Figure 11c illustrates the shape recovery process of bionic SMPC tracheal stents within the magnetic field. The findings revealed that the stent could completely restore its original shape and conform to the trachea model's outer wall, effectively exhibiting minimally invasive implantation properties. Pandey et al.^[153] obtained an SMPC tracheal stent by printing shape-memory PLA/PCL mixture via direct ink writing method. When the mass fractions of PLA and PCL were 70 and 30%, respectively, the obtained tracheal stent was able to completely fit the tracheal lumen under the thermal stimulus and showed good implantable characteristics.

4.3. Intestinal Stent

Stent placement is an effective method of relieving intestinal obstruction.^[154] Self-expanding metallic stents have been widely used to dilate the narrowed intestinal lumen and are categorized into uncoated metallic stents and partially/fully coated metallic stents.^[155] However, metal stents still have many problems, such as uncoated metal stents are prone to mucosal hyperplasia, re-obstruction, and secondary surgery, while coated stents can partially alleviate the aforementioned problems but lead to a significant increase in the risk of dislocation. To solve the problems

of metal stents, biodegradable SMP and SMPC stents have been developed, which have good biocompatibility and low tissue irritation and can avoid the reinfarction problems easily caused by non-biodegradable metal stents.

SMPU, as a classical multiblock SMP, has been widely used in the field of intestinal stents thanks to its excellent mechanical properties, good biocompatibility, and outstanding molecular tailoring ability. Yang et al.^[156] synthesized biodegradable SMPUs and incorporated oxidized carbon black (OCB) with photothermal conversion capabilities to impart near-infrared-responsive shape-memory properties to the SMPUs. The obtained SMPU/OCB composites have tunable chymotrypsin degradation rates and thus have promising applications in intestinal scaffolds.

Biofragmentable anastomotic rings are an ideal sutureless intestinal connecting stent often required in colon surgery. Peng et al.^[157] processed an intestinal anastomotic ring with shape memory based on the mixture of shape-memory PLA and PLGA. By adjusting the mixing ratio of PLA and PLGA, a balance between shape memory and biodegradation can be achieved. The intestinal anastomosis ring, comprising an inner and outer ring, is shown in operation in Figure 12a. Owing to the shape-memory effect, the anastomotic ring can recover from a compressed shape, which simplifies insertion to its original shape for attachment and support. The experimental validation of the intestinal anastomosis ring in porcine intestinal anastomosis is shown in Figure 12b. After resection of the intestinal canal around the tumor, the anastomotic ring was inserted into the intestine and connected by a snap hook structure. After anastomosis, the loop channel ensured the circulation of feces and the anastomotic ring was structurally stable to withstand certain pressure.

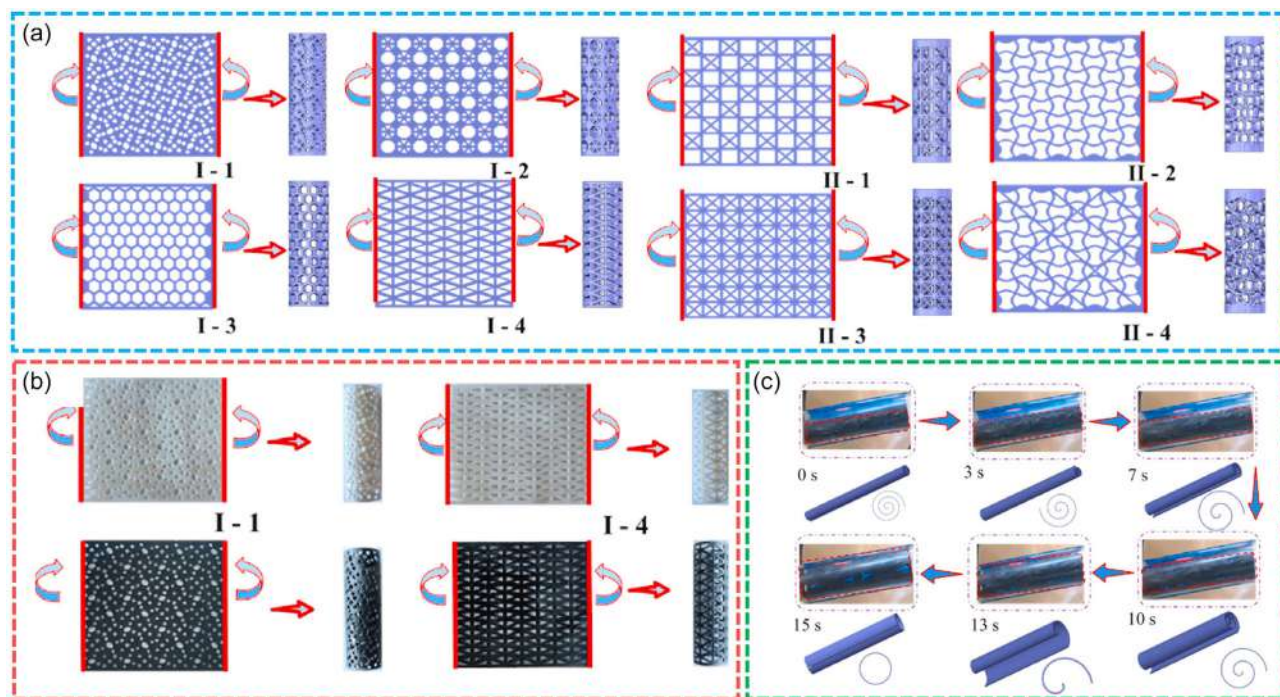


Figure 11. SMPC tracheal stent based on PCL/Fe₃O₄ composite. a) Bionic design of the tracheal stent. b) Unfolded and curled states of the tracheal stent. c) Magnetically driven shape recovery behavior of the tracheal stent. Reproduced with permission.^[40] Copyright 2022, Elsevier.

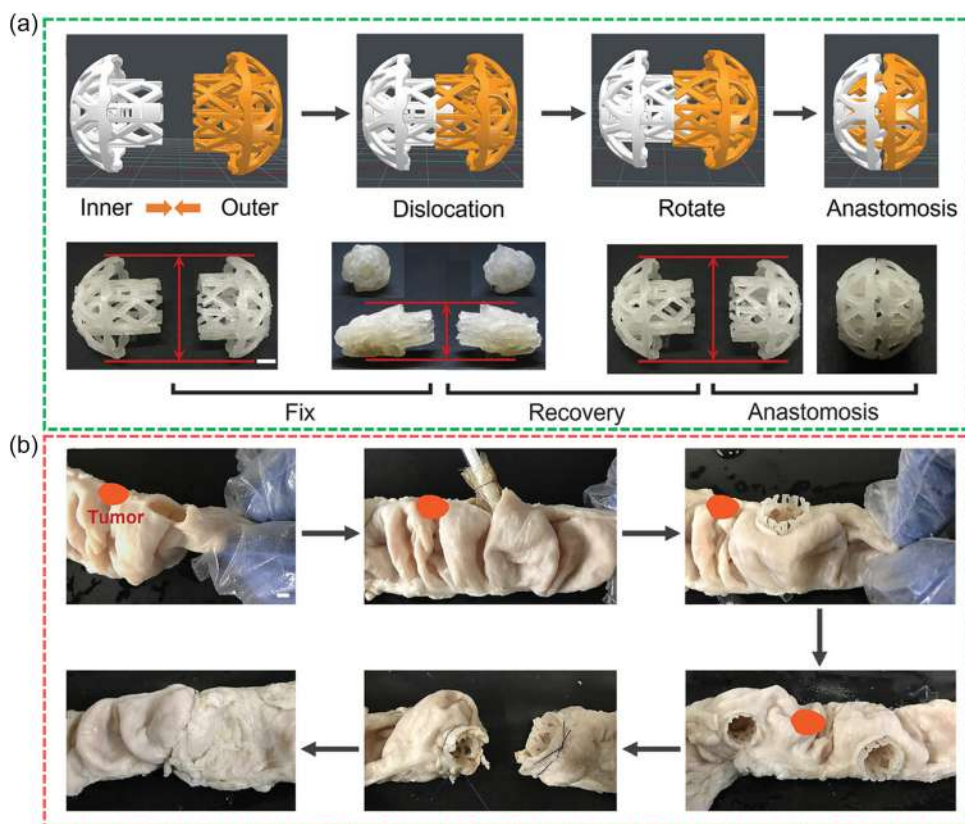


Figure 12. Intestinal anastomotic rings based on shape-memory PLA/PLGA blends. a) Anastomosis process and shape recovery behavior of intestinal anastomotic ring. b) Experimental validation of intestinal anastomosis ring in porcine intestinal anastomosis. Reproduced with permission.^[157] Copyright 2023, Wiley-VCH.

Stent placement is an effective treatment for the relief of malignant colorectal obstruction. Inspired by highly adhesive biological structures in nature (the foot of a gecko, toe pads of a tree frog, and suction cups of an octopus), Lin et al.^[158] developed a colorectal scaffold capable of sustained antitumor and anti-migration properties. PLA/PU/pharmaceutical composites were used in the preparation of colorectal stents to achieve desirable biocompatibility and pliability. Moreover, the colorectal stents were functionalized using graphene oxide to achieve the conversion of near-infrared light energy to thermal energy at the tumor site to complete the photothermal treatment of the tumor. Finally, the effectiveness of the bioinspired colorectal stent to expand the obstructed colon and the feasibility of transanal placement were verified by performing stent implantation experiments on rabbits and pigs.

5. Application in Drug Delivery Carriers

The combination of drug delivery with SMP/SMPC is of great interest because the drug delivery carrier can be easily immobilized at the target site by the shape-memory effect without external manipulation.^[159–161] Moreover, the controllable shape-memory effect allows for prolonged drug release at the target site without the need for multiple injections or surgeries.^[162] In the

field of drug delivery, water actuation is currently considered a more suitable method for SMP/SMPC applications. Fang et al.^[163] developed a shape-memory PVA with a surface strategically coated with SiO₂ nanoparticles to achieve a water-responsive shape-memory effect. By adjusting the coating weight and area of SiO₂, the water-responsive shape-memory PVA demonstrated programmable multistep shape recovery behavior. Utilizing this programmable water-responsive shape-memory PVA, a spiral drug delivery device was created, which releases the drug upon exposure to water (Figure 13a). Similarly, Melocchi et al.^[164] designed an expandable drug delivery system for gastric retention using pharmaceutical-grade PVA, which reverts to its original shape when exposed to an aqueous liquid at 37 °C. The prototypes of the expandable drug delivery system with different original configurations were manually assigned to temporary shapes and inserted into gelatin capsules (Figure 13b). Water-induced shape recovery and release properties were characterized for prototypes with temporary configurations, and satisfactory recovery of the original cylindrical, conical spiral, and S shapes was achieved within a few minutes.

Similarly, Uboldi et al.^[165] designed a retentive drug delivery system based on medical shape-memory PVA. Coatings with different permeability were employed to limit the interaction of the shape-memory PVA matrix with aqueous fluids to prolong the drug release time. Bil et al.^[166] synthesized SMPUs incorporating

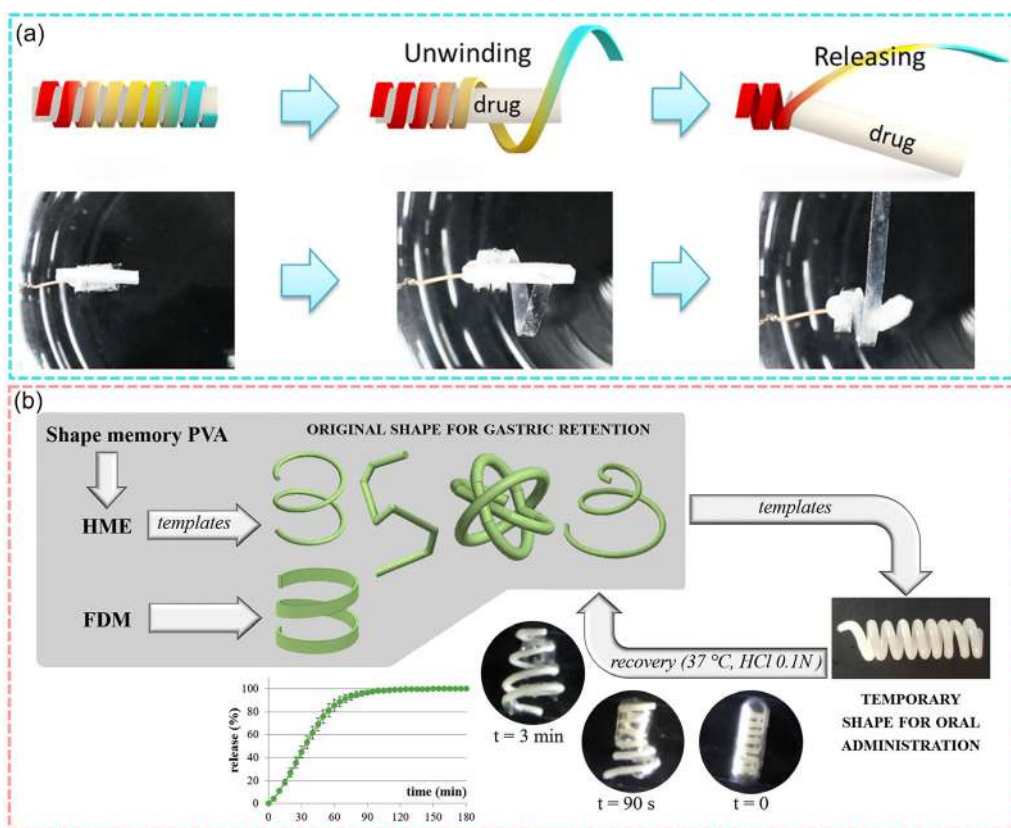


Figure 13. SMP-based water-responsive drug delivery/release carriers. a) Spiral drug release device. Reproduced with permission.^[163] Copyright 2017, American Chemical Society. b) Expandable drug delivery system for gastric retention. Reproduced with permission.^[164] Copyright 2019, Elsevier.

D,L-lactide-*co*-glycolide (*o*-PLGA) or poly-L-lactide diol (oPLLA) to create a material that combines multiple shape memory, biodegradable, and sustained drug delivery properties. Subsequently, they developed a biomaterial consisting of chitosan microspheres (CH-M) and a cross-linked polyester-PU (3b-PU) matrix with shape-memory properties, which enabled controlled drug delivery.^[167] The drug delivery properties of the CH-M/3b-PU composite were assessed *in vitro* using the drug ciprofloxacin hydrochloride (Cpx-HCl), and the results verified the efficacy of the composite as a controllable drug delivery carrier under various pH conditions.

Inverardi et al.^[168] proposed a shape-memory PVA-based drug delivery system for gastric retention, which had an initial S-shaped configuration. It was then programmed to a temporary shape in the form of a planar paper clip in a high-temperature environment at 60 °C. This programming process was achieved by inserting the sample into a pre-designed high-temperature resistant template (Figure 14a). Inspired by the body configuration of *Asterias rubens* during hunting, Heunis et al.^[42] designed a magnetic gastrointestinal drug delivery carrier based on a temperature-sensitive mechanism. An SMP with a low transition temperature was used as a drug carrier to achieve a controlled thermotropic shape transition. Figure 14b shows a schematic diagram of the composition of the *Asterias rubens*-inspired gastrointestinal drug delivery carrier. The carrier consists of a polydimethylsiloxane membrane and an SMP layer, and a

nickel-plated neodymium magnet is fixed in the middle of the SMP layer to guide the device to the target site via a magnetic field. The thermal response characteristics of the drug delivery carrier were assessed using an *in vitro* model, and the findings verified its ability to deliver the drug to the targeted location within a colon model.

To overcome the application limitations of poorly water-soluble materials such as luteolin in the treatment of gastric cancer, a shape-memory PLA-based gastric retention drug delivery system (GRDDS) has recently been developed (Figure 15a).^[169] This GRDDS can improve the relative bioavailability of luteolin and extend its release and *in vivo* circulation time, offering a potential strategy for practical oral drug administration. King et al.^[170] fabricated porous drug-loaded scaffolds using digital light processing 4D printing (Figure 15b). The drug release profiles demonstrated that the scaffolds could achieve tunable and controlled drug release. Over 2 weeks using mouse fibroblasts, the scaffolds exhibited proven cytocompatibility.

6. Challenges and Future Opportunities

Despite the extensive research and significant progress made in the preemptive use of traditional polymers in biomedical devices such as bone tissue scaffolds, lumen stents, and drug delivery carriers, there remain substantial challenges that hinder

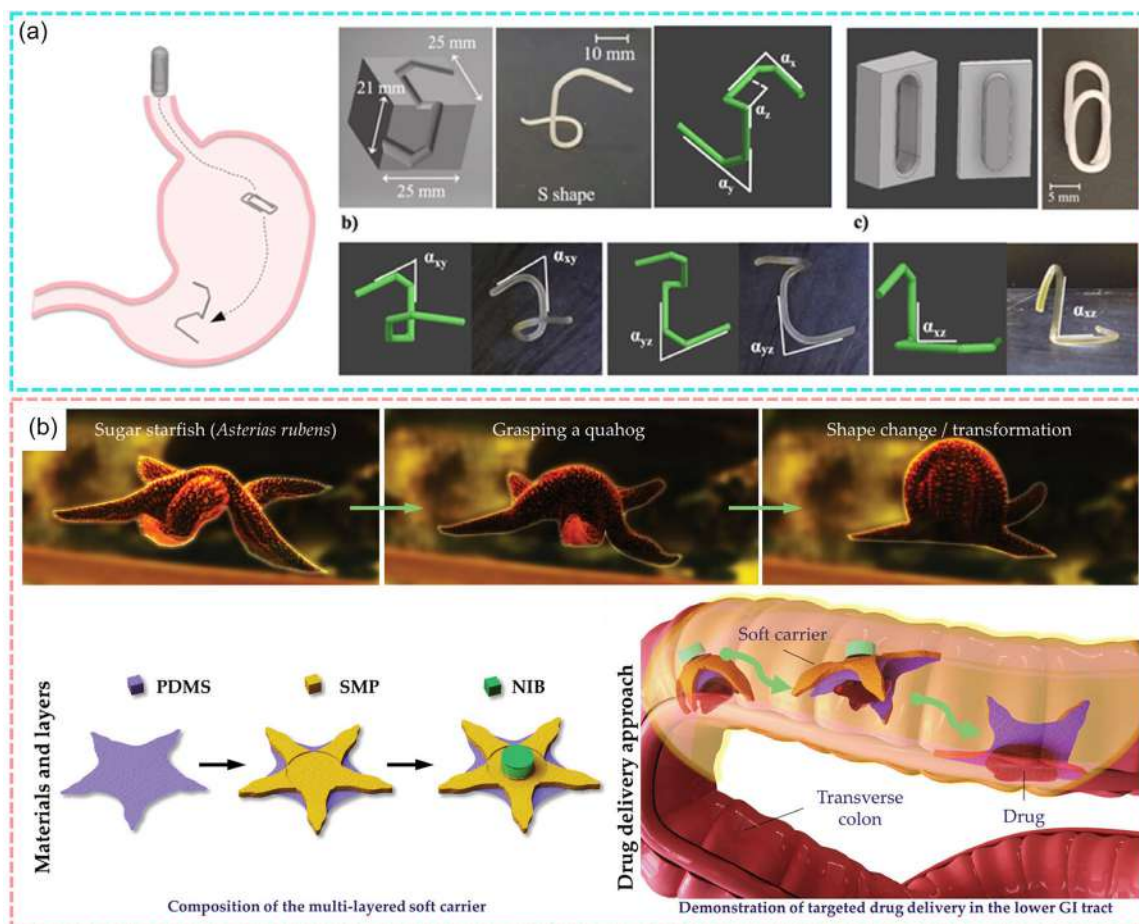


Figure 14. SMP-based thermo-responsive drug delivery carriers. a) Retentive drug delivery system. Reproduced with permission.^[168] Copyright 2021, Elsevier. b) *Asterias rubens*-inspired temperature-controlled gastrointestinal drug delivery device. Reproduced with permission.^[42] Copyright 2023, Wiley-VCH.

their widespread application in clinical therapies. These challenges include biocompatibility issues, long-term stability, and the need for precise control over the material properties to ensure optimal performance. However, the emergence of SMPs and SMPCs has opened up new avenues for addressing these challenges and expanding the possibilities in biomedical applications.

SMPs and SMPCs have garnered significant attention in the field of biomedicine due to their unique shape-memory properties, which encompass shape fixation, shape recovery, and shape adaptation. These properties enable them to meet the specific functional requirements of innovative surgical and medical devices, offering enhanced flexibility, adaptability, and customization. The high design versatility of biomedical shape-memory materials allows for the development of a wide range of biomedical devices tailored to various applications, from minimally invasive surgical tools to personalized implants and smart drug delivery systems.

One of the key advantages of SMPs and SMPCs is their ability to respond to various stimuli beyond temperature, such as pH, solution, light, or even multi-physical fields. This responsiveness enables the creation of intelligent and dynamic biomedical

devices that can adapt to the changing physiological environment and provide targeted and controlled therapeutic interventions. For instance, pH-responsive SMPs can be utilized for drug delivery systems that release drugs specifically in the acidic tumor microenvironment, while light-responsive SMPs can be employed for minimally invasive surgical procedures with precise spatial and temporal control. Furthermore, the continuous advancements in the fabrication methods of SMPs and SMPCs have unlocked new possibilities for personalized treatment approaches. With the adaptive design of the deformation properties of these materials, it is envisioned that patient-specific devices and implants can be developed, taking into account individual anatomical variations and pathological conditions. This personalized approach has the potential to revolutionize healthcare by improving treatment outcomes, reducing complications, and enhancing patient comfort and satisfaction.

However, to fully realize the potential of SMPs and SMPCs in biomedical applications, several challenges need to be addressed. These include the optimization of biocompatibility and biodegradability, ensuring long-term stability and durability, and developing scalable and cost-effective manufacturing processes. Additionally, rigorous *in vitro* and *in vivo* studies are necessary to

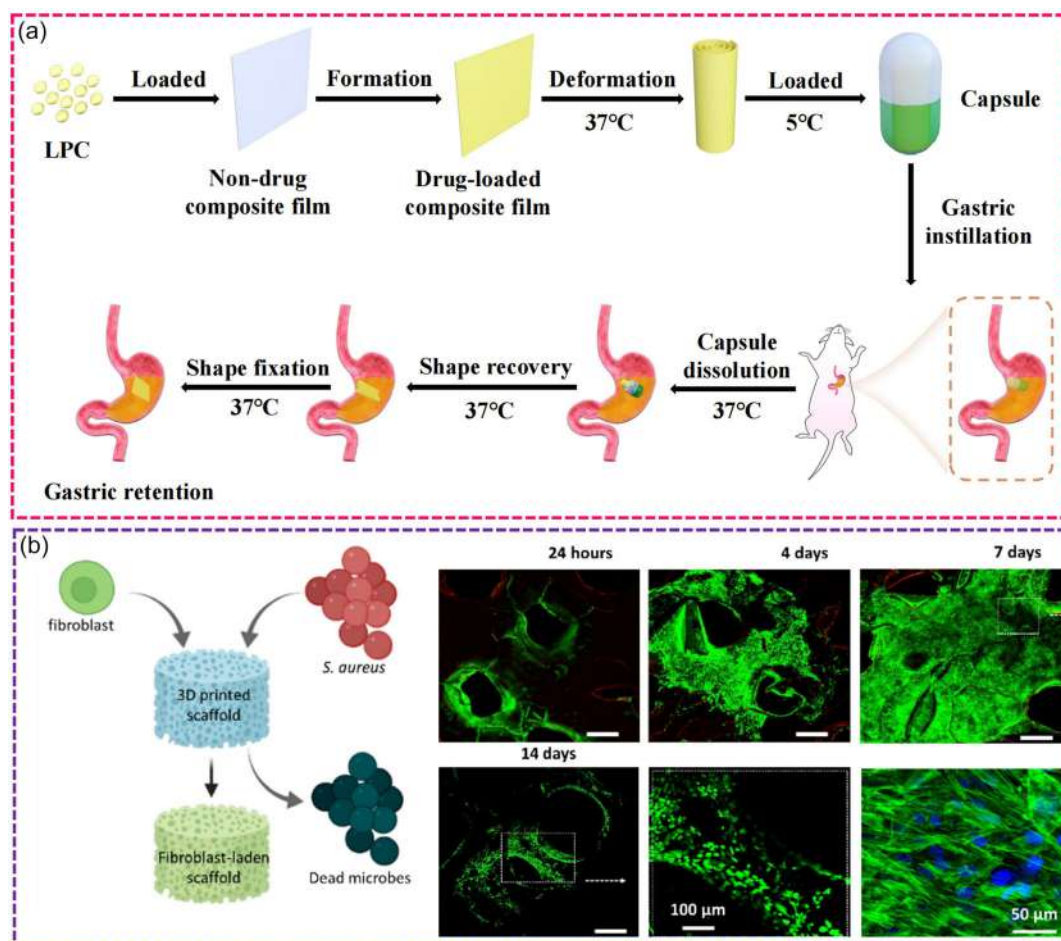


Figure 15. a) Schematic illustration of the PLA-based GRDDS. Reproduced with permission.^[169] Copyright 2024, Elsevier. b) Schematic of cytocompatibility of 4D-printed prodrug scaffolds and results of cell culture experiments. Reproduced with permission.^[170] Copyright 2024, American Chemical Society.

thoroughly evaluate the safety and efficacy of these materials before their translation into clinical practice.

In conclusion, while traditional polymers have laid the foundation for biomedical devices, SMPs and SMPCs offer unparalleled opportunities for the development of next-generation biomedical solutions. With their unique shape-memory properties, responsiveness to various stimuli, and the potential for personalized treatment, these materials hold immense promise for revolutionizing healthcare delivery. As research efforts continue to address the existing challenges and explore new frontiers, it is anticipated that SMPs and SMPCs will play an increasingly crucial role in advancing biomedical technologies, ultimately leading to improved patient outcomes and quality of life in a cost-effective, nontoxic, and efficient manner.

Acknowledgements

This work was financially supported by the National Key R&D Program of China (grant no. 2022YFB3805700) and the National Natural Science Foundation of China (grant no. 12402160).

Conflict of Interest

The authors declare no conflict of interest.

Author Contributions

Chengjun Zeng: conceptualization (lead); funding acquisition (equal); resources (equal); validation (equal); and writing—original draft (lead). **Liwu Liu:** conceptualization (equal); methodology (equal); visualization (lead); and writing—review and editing (equal). **Wei Zhao:** formal analysis (lead); investigation (equal); and writing—review and editing (equal). **Xiaozhou Xin:** investigation (equal); methodology (equal); and writing—review and editing (equal). **Yanju Liu:** investigation (equal); project administration (lead); supervision (equal); and writing—review and editing (equal). **Jinsong Leng:** methodology (equal); supervision (lead); and writing—review and editing (equal).

Keywords

4D printings, bone tissue scaffolds, drug delivery devices, shape-memory polymer composites, vascular stents

Received: September 12, 2024

Revised: December 13, 2024

Published online:

- [1] D. Ravichandran, M. Kakarla, W. Xu, S. Jambhulkar, Y. Zhu, M. Bawareth, N. Fonseca, D. Patil, K. Song, *Compos. Part B Eng. Mater.* **2022**, *247*, 110352.
- [2] C. Zeng, L. Liu, Y. Hu, W. Zhao, X. Xin, Y. Liu, J. Leng, *Adv. Funct. Mater.* **2024**, *34*, 2408887.
- [3] C. Zeng, L. Liu, X. Xin, W. Zhao, C. Lin, Y. Liu, J. Leng, *Compos. Sci. Technol.* **2024**, *249*, 110503.
- [4] W. Zhang, C. Zou, Q. Pan, G. Hu, H. Shi, Y. Zhang, X. He, Y. He, X. Zhang, *Adv. Funct. Mater.* **2024**, *34*, 2400245.
- [5] C. Zeng, L. Liu, W. Bian, J. Leng, Y. Liu, *Compos. Struct.* **2022**, *280*, 114952.
- [6] A. Sheikh, M. A. S. Abourehab, P. Kesharwani, *Drug. Discov. Today* **2023**, *28*, 103391.
- [7] H. Li, B. Zhang, H. Ye, B. Jia, X. He, J. Cheng, Z. Sun, R. Wang, Z. Chen, J. Lin, R. Xiao, Q. Liu, Q. Ge, *Sci Adv.* **2024**, *10*, ead14387.
- [8] S. Feng, X. Peng, J. Cui, R. Feng, Y. Sun, Y. Guo, Z. Lu, W. Gao, F. Liu, C. Liang, G. Hu, B. Zhang, *Adv. Funct. Mater.* **2024**, 2401431.
- [9] J. Huang, Y. Jiang, Q. Chen, H. Xie, S. Zhou, *Nat. Commun.* **2023**, *14*, 7131.
- [10] X. Wang, Y. He, Y. Liu, J. Leng, *Mater. Sci. Eng. R: Rep.* **2022**, *151*, 100702.
- [11] Y. Xia, Y. He, F. Zhang, Y. Liu, J. Leng, *Adv. Mater.* **2021**, *33*, e2000713.
- [12] S. Yan, F. Zhang, L. Luo, L. Wang, Y. Liu, J. Leng, *Research* **2023**, *6*, 0234.
- [13] C. Strutyński, M. Evrard, F. Désévéday, G. Gadret, J.-C. Jules, C.-H. Brachais, B. Kibler, F. Smektala, *Nat. Commun.* **2023**, *14*, 6561.
- [14] W. Zhao, N. Li, L. Liu, J. Leng, Y. Liu, *Appl. Phys. Rev.* **2023**, *10*, 011306.
- [15] J. Chen, Z. Wang, B. Yao, Y. Geng, C. Wang, J. Xu, T. Chen, J. Jing, J. Fu, *Adv. Mater.* **2024**, *36*, 2401178.
- [16] W. Zhao, C. Yue, L. Liu, Y. Liu, J. Leng, *Adv. Healthcare Mater.* **2022**, e2201975.
- [17] E. Kuram, H. H. Karadeli, *Macromol. Rapid Commun.* **2024**, *45*, 2400146.
- [18] C. Zeng, L. Liu, Y. Du, M. Yu, X. Xin, T. Liu, P. Xu, Y. Yan, D. Zhang, W. Dai, X. Lan, F. Zhang, L. Wang, X. Wan, W. Bian, Y. Liu, J. Leng, *Engineering* **2023**, *28*, 49.
- [19] C. Zeng, L. Liu, Y. Du, M. Yu, X. Xin, P. Xu, F. Li, L. Wang, F. Zhang, Y. Liu, J. Leng, *Compos. Commun.* **2023**, *42*, 101690.
- [20] P. Wu, T. Yu, M. Chen, N. Kang, M. E. Mansori, *Adv. Funct. Mater.* **2024**, *34*, 2314854.
- [21] C. Zeng, L. Liu, C. Lin, X. Xin, Y. Liu, J. Leng, *Compos. Part A* **2024**, *180*, 108085.
- [22] H. Yang, R. Shi, Q. Jiang, J. Ren, *Adv. Compos. Hybrid Mater.* **2022**, *6*, 1.
- [23] Y. Lu, Y. Wu, J. Wu, P. Yang, Y. Zhang, W. Zhao, X. Zhang, Z. Cui, P. Fu, X. Pang, M. Liu, *J. Mater. Res. Technol.* **2024**, *29*, 2062.
- [24] R. E. Booth, C. Khanna, H. M. Schrickx, S. Siddika, A. Al Shafe, B. T. O'Connor, *ACS Appl. Mater. Interfaces* **2022**, *14*, 53129.
- [25] S. Yu, N. Sadaba, E. Sanchez-Rexach, S. L. Hilburg, L. D. Pozzo, G. Altin-Yavuzarslan, L. M. Liz-Marzán, D. Jimenez de Aberasturi, H. Sardon, A. Nelson, *Adv. Funct. Mater.* **2023**, *34*, 2311209.
- [26] K. Boga, A. F. Patti, J. C. Warner, G. P. Simon, K. Saito, *Compos. Commun.* **2023**, *44*, 101740.
- [27] V. Chalut, D. Le Roy, T. Mercier, M. C. Audry, V. Vieille, T. Devillers, A. L. Deman, C. Tomba, *Small Sci.* **2024**, 2400141.
- [28] C. Lin, X. Xin, L. Tian, D. Zhang, L. Liu, Y. Liu, J. Leng, *Compos. Part B Eng.* **2024**, *274*, 111257.
- [29] M. Y. Khalid, Z. U. Arif, R. Noroozi, A. Zolfagharian, M. Bodaghi, *J. Manuf. Process.* **2022**, *81*, 759.
- [30] L. Zhang, X. Li, E. Ding, Z. Guo, C. Luo, H. Zhang, J. Yu, *Compos. Sci. Technol.* **2024**, *251*, 110588.
- [31] H. Hassan, H. Hallez, W. Thielemans, V. Vandeginste, *Eur. Polym. J.* **2024**, *208*, 112861.
- [32] M. Y. Khalid, Z. U. Arif, A. Tariq, M. Hossain, K. Ahmed Khan, R. Umer, *Eur. Polym. J.* **2024**, *205*, 112718.
- [33] C. Lin, Z. Huang, Q. Wang, Z. Zou, W. Wang, L. Liu, Y. Liu, J. Leng, *Compos. Part B Eng.* **2023**, *256*, 110623.
- [34] M. A. Kouka, F. Abbassi, M. Habibi, F. Chabert, A. Zghal, C. Garnier, *Adv. Eng. Mater.* **2022**, *25*, 2200650.
- [35] S. A. Pineda-Castillo, T. L. Cabaniss, H. Aboukeila, B. P. Grady, H. Lee, B. N. Bohnstedt, Y. Liu, C.-H. Lee, *Adv. Eng. Mater.* **2023**, *25*, 300683.
- [36] J. Hu, Y. Zhu, H. Huang, J. Lu, *Prog. Polym. Sci.* **2012**, *37*, 1720.
- [37] Y. Zhu, J. L. Hu, K. W. Yeung, Y. Q. Liu, H. M. Liem, *J. Appl. Polym. Sci.* **2006**, *100*, 4603.
- [38] D. Zhang, W. L. Burkes, C. A. Schoener, M. A. Grunlan, *Polymer* **2012**, *53*, 2935.
- [39] W. Zhao, Z. Huang, L. Liu, W. Wang, J. Leng, Y. Liu, *Compos. Sci. Technol.* **2021**, *203*, 108563.
- [40] W. Zhao, Z. Huang, L. Liu, W. Wang, J. Leng, Y. Liu, *Compos. Sci. Technol.* **2022**, *229*, 109671.
- [41] C. Lin, J. Lv, Y. Li, F. Zhang, J. Li, Y. Liu, L. Liu, J. Leng, *Adv. Funct. Mater.* **2019**, *29*, 1906569.
- [42] C. M. Heunis, Z. Wang, G. de Vente, S. Misra, V. K. Venkiteswaran, *Macromol Biosci.* **2023**, *23*, 2200559.
- [43] Y. Zhang, J. Hu, R. Xie, Y. Yang, J. Cao, Y. Tu, Y. Zhang, T. Qin, X. Zhao, *Acta Biomater.* **2020**, *103*, 293.
- [44] X. Wan, H. Wei, F. Zhang, Y. Liu, J. Leng, *J. Appl. Polym. Sci.* **2019**, *136*, 48177.
- [45] H. Wu, H. Wu, Y. Liu, J. Hu, N. Zhang, X. Wu, Z. Sun, G. Wei, Y. Chen, Y. Duan, J. Zhang, *Compos. Sci. Technol.* **2023**, *239*, 110064.
- [46] R. Scaffaro, A. Maio, F. Sutura, E. F. Gulino, M. Morreale, *Polymers* **2019**, *11*, 651.
- [47] M. Gharibshahian, M. Salehi, N. Beheshtizadeh, M. Kamalabadi-Farahani, A. Atashi, M.-S. Nourbakhsh, M. Alizadeh, *Front. Bioeng. Biotechnol.* **2023**, *11*, 1168504.
- [48] A. Kurowska, A. Nikodem, A. Jabłoński, J. Janusz, P. Szczygieł, M. Ziabka, E. Menaszek, M. Dziadek, B. Zagrajczuk, M. Kobielarz, I. Rajzer, *Mater. Design* **2023**, *233*, 112255.
- [49] L. Wu, L. Bao, Z. Wang, Z. Yu, B. Wang, Q. Chen, Y. Ling, Y. Qin, K. Tang, Y. Cai, R. Huang, *Adv. Electron. Mater.* **2021**, *7*, 2001104.
- [50] Z. Miri, S. Farè, Q. Ma, H. J. Haugen, *Prog. Biomed. Eng.* **2023**, *5*, 042001.
- [51] H.-R. Yang, G. Jia, H. Wu, C. Ye, K. Yuan, S. Liu, L. Zhou, H. Xu, L. Gao, J. Cui, S. Fang, *Mater. Lett.* **2022**, *329*, 133067.
- [52] S. Sarfraz, A. M. Tamminen, J. Leikola, S. Salmi, M. Kaakinen, T. Sorsa, J. Suojanen, J. Reunanen, *Int. J. Mol. Sci.* **2023**, *24*, 9504.
- [53] S. Zhou, J. Cui, M. Fang, Y. Ke, Y. Jiang, H. Jia, X. Zhu, X. Yin, *J. Cleaner Prod.* **2024**, *479*, 144044.
- [54] S. Sitthisang, X. Hou, A. Treetong, X. Xu, W. Liu, C. He, U. Sae-Ueng, S. Yodmuang, *Sci. Rep.* **2024**, *14*, 21097.
- [55] B. Tyler, D. Gullotti, A. Mangraviti, T. Utsuki, H. Brem, *Adv. Drug Delivery Rev.* **2016**, *107*, 163.
- [56] S. Jayalath, E. Trifoni, J. Epaarachchi, M. Herath, E. E. Gdoutos, B. Samarasekera, *Compos. Sci. Technol.* **2024**, *258*, 110870.
- [57] L. Zhang, K. Jiang, R. Tao, Y. Mao, S. Hou, *Compos. Struct.* **2024**, *331*, 117837.
- [58] H. Lee, Y. Jang, Y. W. Chang, C. Lim, *Polymers* **2024**, *16*, 2714.
- [59] X. Cheng, Y. Chen, S. Dai, M. M. M. Bilek, S. Bao, L. Ye, *J. Mech. Behav. Biomed. Mater.* **2019**, *100*, 103372.

- [60] A. Fallah, S. Asif, G. Gokcer, B. Koc, *Compos. Struct.* **2023**, 316, 117034.
- [61] M. Lalegani Dezaki, M. Bodaghi, *Eur. Polym. J.* **2024**, 210, 112988.
- [62] H.-J. Um, J.-S. Lee, J.-H. Shin, H.-S. Kim, *Compos. Struct.* **2022**, 291, 115590.
- [63] H. Xie, J. Shao, Y. Ma, J. Wang, H. Huang, N. Yang, H. Wang, C. Ruan, Y. Luo, Q. Q. Wang, P. K. Chu, X. F. Yu, *Biomaterials* **2018**, 164, 11.
- [64] M. Kim, Y. B. Kim, H. J. Chun, *Polym. Adv. Technol.* **2024**, 35, e6257.
- [65] M. Li, K. Chen, D. Zhang, Z. Ye, Z. Yang, Q. Wang, Z. Jiang, Y. Zhang, Y. Shang, A. Cao, *Adv. Sci.* **2024**, 11, e2404913.
- [66] M. Zare, N. Parvin, M. P. Prabhakaran, J. A. Mohandes, S. Ramakrishna, *Compos. Sci. Technol.* **2019**, 184, 107874.
- [67] M. Hanif, L. Zhang, A. H. Shah, Z. Chen, *Addit. Manuf.* **2024**, 86, 104174.
- [68] Y. Guo, X. An, X. Qian, *Ind. Crop. Prod.* **2023**, 193, 116247.
- [69] S. Choudhury, A. Joshi, D. Dasgupta, A. Ghosh, S. Asthana, K. Chatterjee, *Mater. Adv.* **2024**, 5, 3345.
- [70] W. Guo, B. Zhou, Y. Zou, X. Lu, *Adv. Eng. Mater.* **2023**, 26, 2301381.
- [71] S. Selçuk Pekdemir, H. Onay, E. Özen Öner, M. E. Pekdemir, M. Kök, B. Ateş, Y. Aydoğdu, G. Dalğıç, *J. Appl. Polym. Sci.* **2024**, 141, e55187.
- [72] Y. Wang, L. Huang, X. Wang, X. Lu, B. Wang, Y. Qin, C. Huang, *Polym. Test* **2023**, 120, 107966.
- [73] R. Du, B. Zhao, K. Luo, M.-X. Wang, Q. Yuan, L.-X. Yu, K.-K. Yang, Y.-Z. Wang, *ACS Appl. Mater. Interfaces* **2023**, 15, 42930.
- [74] F. O. Beltran, A. S. Arabiyat, R. A. Culibrk, D. J. Yeisley, C. J. Houk, A. J. Hicks, J. Negrón Hernández, B. M. Nitschke, M. S. Hahn, M. A. Grunlan, *Polymer* **2023**, 284, 126291.
- [75] G. Li, Z. Li, Y. Min, S. Chen, R. Han, Z. Zhao, *Small* **2023**, 19, 2302927.
- [76] X. Chen, Z. Huang, Q. Yang, X. Zeng, R. Bai, L. Wang, *Biomed. Mater.* **2022**, 17, 065022.
- [77] C. Shuai, Z. Wang, S. Peng, Y. Shuai, Y. Chen, D. Zeng, P. Feng, *Mater. Chem. Front.* **2022**, 6, 1456.
- [78] X. Xu, J. D. Skelly, J. Song, *ACS Appl. Mater. Interfaces* **2023**, 15, 2693.
- [79] Y. Wang, H. Cui, T. Esworthy, D. Mei, Y. Wang, L. G. Zhang, *Adv. Mater.* **2022**, 34, e2109198.
- [80] Y. S. Alshebly, M. Nafea, M. S. Mohamed Ali, H. A. F. Almurib, *Eur. Polym. J.* **2021**, 159, 110708.
- [81] Z. Mao, X. Bi, C. Yu, L. Chen, J. Shen, Y. Huang, Z. Wu, H. Qi, J. Guan, X. Shu, B. Yu, Y. Zheng, *Nat. Commun.* **2024**, 15, 4160.
- [82] Y. Piskarev, Y. Sun, M. Righi, Q. Boehler, C. Chautems, C. Fischer, B. J. Nelson, J. Shintake, D. Floreano, *Adv. Sci.* **2024**, 11, 2305537.
- [83] X. Guo, X. Wang, H. Tang, Y. Ren, D. Li, B. Yi, Y. Zhang, *ACS Appl. Mater. Interfaces* **2022**, 14, 23219.
- [84] Z. Deng, Y. Guo, X. Zhao, L. Li, R. Dong, B. Guo, P. X. Ma, *Acta Biomater.* **2016**, 46, 234.
- [85] S. Chayanun, A. A. Soufivand, J. Faber, S. Budday, B. Lohwongwatana, A. R. Boccaccini, *Adv. Eng. Mater.* **2024**, 26, 2300641.
- [86] Y. Zhu, J. Zhou, B. Dai, W. Liu, J. Wang, Q. Li, J. Wang, L. Zhao, T. Ngai, *Adv. Healthcare Mater.* **2022**, 11, 2201679.
- [87] K. K. Moncal, R. S. Tigli Aydın, K. P. Godzik, T. M. Aciri, D. N. Heo, E. Rizk, H. Wee, G. S. Lewis, A. K. Salem, I. T. Ozbolat, *Biomaterials* **2022**, 281, 121333.
- [88] Y. Shi, L. Wang, L. Sun, Z. Qiu, X. Qu, J. Dang, Z. Zhang, J. He, H. Fan, *Int. J. Bioprinting* **2023**, 9, 1071.
- [89] Y. Zhao, W. Sun, X. Wu, X. Gao, F. Song, B. Duan, A. Lu, H. Yang, C. Huang, *ACS Nano* **2024**, 18, 7204.
- [90] W. Jiang, Y. Zhan, Y. Zhang, D. Sun, G. Zhang, Z. Wang, L. Chen, J. Sun, *Biomaterials* **2024**, 308, 122566.
- [91] D. Zhang, O. J. George, K. M. Petersen, A. C. Jimenez-Vergara, M. S. Hahn, M. A. Grunlan, *Acta Biomater.* **2014**, 10, 4597.
- [92] X. Liu, K. Zhao, T. Gong, J. Song, C. Bao, E. Luo, J. Weng, S. Zhou, *Biomacromolecules* **2014**, 15, 1019.
- [93] R. Xie, J. Hu, F. Ng, L. Tan, T. Qin, M. Zhang, X. Guo, *Ceram. Int.* **2017**, 43, 4794.
- [94] L. Wang, X. Chen, X. Zeng, K. Luo, S. Zhou, P. Zhang, J. Li, *Compos. Sci. Technol.* **2022**, 217, 109124.
- [95] J. Yu, H. Xia, A. Teramoto, Q. Q. Ni, *J. Biomed. Mater. Res. A* **2017**, 105, 1132.
- [96] C. Shuai, W. Xu, H. He, F. Yang, J. Liu, P. Feng, *J. Mater. Res. Technol.* **2024**, 30, 61.
- [97] C. Shuai, Z. Wang, F. Yang, H. Zhang, J. Liu, P. Feng, *J. Adv. Res.* **2024**, 65, 167.
- [98] F. Yang, X. Jia, C. Hua, F. Zhou, J. Hua, Y. Ji, P. Zhao, Q. Yuan, M. Xing, G. Lyu, *Bioact. Mater.* **2024**, 36, 30.
- [99] J. Song, J. Dong, Z. Yuan, M. Huang, X. Yu, Y. Zhao, Y. Shen, J. Wu, M. El-Newehy, M. M. Abdulhameed, B. Sun, J. Chen, X. Mo, *Adv. Healthcare Mater.* **2024**, 13, 2401160.
- [100] L. Van Daele, V. Chausse, L. Parmentier, J. Brancart, M. Pegueroles, S. Van Vlierberghe, P. Dubruel, *Adv. Healthcare Mater.* **2024**, 13, 2303498.
- [101] R. M. Baker, L. F. Tseng, M. T. Iannolo, M. E. Oest, J. H. Henderson, *Biomaterials* **2016**, 76, 388.
- [102] Y. Zhang, C. Li, W. Zhang, J. Deng, Y. Nie, X. Du, L. Qin, Y. Lai, *Bioact. Mater.* **2022**, 16, 218.
- [103] S. Zhou, Z. Bei, J. Wei, X. Yan, H. Wen, Y. Cao, H. Li, *J. Mater. Chem. B* **2022**, 10, 1019.
- [104] C. Cheng, X. Peng, Y. Luo, S. Shi, L. Wang, Y. Wang, X. Yu, *J. Mater. Chem. B* **2023**, 11, 10464.
- [105] Y. Deng, F. Zhang, Y. Liu, S. Zhang, H. Yuan, J. Leng, *ACS Appl. Polym. Mater.* **2023**, 5, 1283.
- [106] K. Luo, P. Gao, W. Yang, X. Lei, T.-W. Wong, A. F. Ismail, L. Wang, *Appl. Mater. Today* **2023**, 31, 101752.
- [107] J. Zhang, X. Yang, W. Li, H. Liu, Z. Yin, Y. Chen, X. Zhou, *Compos. Part B Eng.* **2024**, 275, 111346.
- [108] Y. Lyu, D. Liu, R. Guo, Z. Ji, X. Wang, X. Shi, *Polymer* **2023**, 266, 125637.
- [109] K. Saptaji, C. O. Rochmad, O. A. Juniasih, G. K. Sunnardianto, F. Triawan, A. I. Ramadhan, A. Azhari, *Prog. Addit. Manuf.* **2024**, 9, 1869.
- [110] Z. Ren, K. Ding, X. Zhou, T. Ji, H. Sun, X. Chi, M. Xu, *Int. J. Biol. Macromol.* **2023**, 253, 126562.
- [111] F. S. Senatov, K. V. Niaza, M. Y. Zadorozhnyy, A. V. Maksimkin, S. D. Kaloshkin, Y. Z. Estrin, *J. Mech. Behav. Biomed. Mater.* **2016**, 57, 139.
- [112] F. S. Senatov, M. Y. Zadorozhnyy, K. V. Niaza, V. V. Medvedev, S. D. Kaloshkin, N. Y. Anisimova, M. V. Kiselevskiy, K.-C. Yang, *Eur. Polym. J.* **2017**, 93, 222.
- [113] C. Wang, H. Yue, J. Liu, Q. Zhao, Z. He, K. Li, B. Lu, W. Huang, Y. Wei, Y. Tang, M. Wang, *Biofabrication* **2020**, 12, 045025.
- [114] A. K. Singh, K. Pramanik, A. Biswas, *Bio-Des. Manuf.* **2023**, 7, 57.
- [115] A. Maihemuti, H. Zhang, X. Lin, Y. Wang, Z. Xu, D. Zhang, Q. Jiang, *Bioact. Mater.* **2023**, 26, 77.
- [116] O. Yue, X. Wang, M. Hou, M. Zheng, D. Hao, Z. Bai, X. Zou, B. Cui, C. Liu, X. Liu, *Nano Energy* **2023**, 107, 108158.
- [117] F. Zhang, L. Wang, Z. Zheng, Y. Liu, J. Leng, *Compos. Part A* **2019**, 125, 1906657.
- [118] H.-J. Jeong, H. Nam, J.-S. Kim, S. Cho, H.-H. Park, Y.-S. Cho, H. Jeon, J. Jang, S.-J. Lee, *Bioact. Mater.* **2024**, 31, 590.
- [119] S. Ualiyeva, N. Hallen, Y. Kanaoka, C. Ledderose, I. Matsumoto, W. G. Junger, N. A. Barrett, L. G. Bankova, *Sci. Adv.* **2020**, 5, eaax7224.
- [120] K. A. van Kampen, E. Olaret, I.-C. Stancu, L. Moroni, C. Mota, *Mater. Sci. Eng. C* **2021**, 119, 111472.
- [121] Y.-T. Song, L. Dong, J.-G. Hu, P.-C. Liu, Y.-L. Jiang, L. Zhou, M. Wang, J. Tan, Y.-X. Li, Q.-Y. Zhang, C.-Y. Zou, X.-Z. Zhang,

- L.-M. Zhao, R. Nie, Y. Zhang, J. Li-Ling, H.-Q. Xie, *Compos. Part B* **2023**, 250, 110461.
- [122] F. Zhang, N. Wen, L. Wang, Y. Bai, J. Leng, *Int. J. Smart Nano. Mater.* **2021**, 12, 375.
- [123] J. Zong, Q. He, Y. Liu, M. Qiu, J. Wu, B. Hu, *Mater. Today Bio* **2022**, 16, 100368.
- [124] S. Wells, Y. Choi, R. Jackson, M. Parwaiz, S. Mehta, V. Selak, M. Harwood, C. Grey, N. Kerse, K. Poppe, *Age Ageing* **2022**, 51.
- [125] T. J. van Trier, M. Snaterse, S. H. J. Hageman, N. ter Hoeve, M. Sunamura, E. P. Moll van Charante, H. Galenkamp, J. W. Deckers, F. M. A. C. Martens, F. L. J. Visseren, W. J. M. Scholte op Reimer, R. J. G. Peters, H. T. Jørstad, *Eur. J. Prev. Cardiol.* **2023**, 30, 601.
- [126] P. Ameri, E. Bertero, M. Lombardi, I. Porto, M. Canepa, A. Nohria, R. Vergallo, A. R. Lyon, T. López-Fernández, *Eur. Heart J.* **2024**, 45, 1209.
- [127] M. Kalogeropoulou, P. J. Díaz-Payno, M. J. Mirzaali, G. J. V. M. van Osch, L. E. Fratila-Apachitei, A. A. Zadpoor, *Biofabrication* **2024**, 16, 022002.
- [128] A. Mahjoubnia, D. Cai, Y. Wu, S. D. King, P. Torkian, A. C. Chen, R. Talaie, S.-Y. Chen, J. Lin, *Acta Biomater.* **2024**, 177, 165.
- [129] S. Choudhury, A. Joshi, V. S. Baghel, G. K. Ananthasuresh, S. Asthana, S. Homer-Vanniasinkam, K. Chatterjee, *J. Mater. Chem. B* **2024**, 12, 5678.
- [130] C. Pan, X. Liu, Q. Hong, J. Chen, Y. Cheng, Q. Zhang, L. Meng, J. Dai, Z. Yang, L. Wang, *J. Magnes. Alloy* **2023**, 11, 48.
- [131] L. S. Paone, M. Szkolnicki, B. J. DeOre, K. A. Tran, N. Goldman, A. M. Andrews, S. H. Ramirez, P. A. Galie, *ACS Appl. Mater. Interfaces* **2024**, 16, 14457.
- [132] Y. Zhao, Z. Wang, L. Bai, F. Zhao, S. Liu, Y. Liu, X. Yao, R. Hang, *Mater. Sci. Eng. C* **2021**, 123, 112007.
- [133] D. Tyvoll, N. Chen, C. Blanco, *Surf. Coat. Technol.* **2023**, 473, 130031.
- [134] Q. Zhang, Z. Zhao, D. Wu, K. Chen, S. Weng, *Int. J. Mech. Sci.* **2023**, 254, 108405.
- [135] H. Jia, S.-Y. Gu, K. Chang, *Adv. Polym. Technol.* **2018**, 37, 3222.
- [136] C. Lin, L. Zhang, Y. Liu, L. Liu, J. Leng, *Sci. China Technol. Sci.* **2020**, 63, 578.
- [137] S. Shi, M. Cui, F. Sun, K. Zhu, M. I. Iqbal, X. Chen, B. Fei, R. K. Y. Li, Q. Xia, J. Hu, *Adv. Mater.* **2021**, 33, e2101005.
- [138] H. Wei, Q. Zhang, Y. Yao, L. Liu, Y. Liu, J. Leng, *ACS Appl. Mater. Interfaces* **2017**, 9, 876.
- [139] S. Ahmad Zubir, N. Mat Saad, F. W. Harun, E. S. Ali, S. Ahmad, *Polym. Adv. Technol.* **2018**, 29, 2926.
- [140] Z. Li, Z. Chen, Y. Gao, Y. Xing, Y. Zhou, Y. Luo, W. Xu, Z. Chen, X. Gao, K. Gupta, K. Anbalakan, L. Chen, C. Liu, J. Kong, H. L. Leo, C. Hu, H. Yu, Q. Guo, *Biomaterials* **2022**, 283, 121426.
- [141] K. Chen, M. Li, Z. Yang, Z. Ye, D. Zhang, B. Zhao, Z. Xia, Q. Wang, X. Kong, Y. Shang, C. Liu, H. Yu, A. Cao, *Adv. Mater.* **2024**, 36, 2313354.
- [142] Q. Zhang, J. Chen, H. Wang, D. Xie, Z. Yang, J. Hu, H. Luo, Y. Wan, *Macromol. Biosci.* **2024**, 24, 2300401.
- [143] Q. Peng, S. Wang, J. Han, C. Huang, H. Yu, D. Li, M. Qiu, S. Cheng, C. Wu, M. Cai, S. Fu, B. Chen, X. Wu, S. Du, T. Xu, *Research* **2024**, 7, 0339.
- [144] Y. Liu, L. Wang, Z. Liu, Y. Kang, T. Chen, C. Xu, T. Zhu, *ACS Nano* **2023**, 18, 951.
- [145] O. A. Sindeeva, E. S. Prikozhdnenko, I. Schurov, N. Sedykh, S. Goriainov, A. Karamyan, E. A. Mordovina, O. A. Inozemtseva, V. Kudryavtseva, L. E. Shchesnyak, R. A. Abramovich, S. Mikhajlov, G. B. Sukhorukov, *Pharmaceutics* **2021**, 13, 1437.
- [146] M. Singh, D. L. Teodorescu, M. Rowlett, S. X. Wang, M. Balcells, C. Park, B. Bernardo, S. McGarel, C. Reeves, M. R. Mehra, X. Zhao, H. Yuk, E. T. Roche, *Adv. Mater.* **2023**, 36, 2307288.
- [147] Y. Li, M. Li, X. Wang, Y. Wang, C. Li, Y. Zhao, Z. Li, J. Chen, J. Li, K. Ren, Z. Li, J. Ren, X. Han, Q. Li, *Sci. Rep.* **2021**, 11, 23115.
- [148] S. Rodriguez-Zapater, C. Serrano-Casorran, J. A. Guirola, S. Lopez-Minguez, C. Bonastre, M. A. de Gregorio, *Arch. Bronconeumol.* **2020**, 56, 643.
- [149] W. Zhao, N. Li, L. Liu, J. Leng, Y. Liu, *Compos. Struct.* **2022**, 293, 115669.
- [150] M. Zarek, N. Mansour, S. Shapira, D. Cohn, *Macromol. Rapid Commun.* **2017**, 38, 1600628.
- [151] N. Maity, N. Mansour, P. Chakraborty, D. Bychenko, E. Gazit, D. Cohn, *Adv. Funct. Mater.* **2021**, 31, 2108436.
- [152] W. Zhao, F. Zhang, J. Leng, Y. Liu, *Compos. Sci. Technol.* **2019**, 184, 107866.
- [153] H. Pandey, S. S. Mohol, R. Kandi, *Mater. Lett.* **2022**, 329, 133238.
- [154] Y. Feng, Z. Han, C. Chen, X. Wang, J. Liu, Y. Khan, M. Xie, Y. Chen, Y. Zhang, G. Li, *Colloid. Surf. B* **2024**, 233, 113635.
- [155] C. Mu, L. Chen, *Sci. Rep.* **2023**, 13, 1600.
- [156] R. Yang, W. Liu, N. Song, X. Li, Z. Li, F. Luo, J. Li, H. Tan, *Macromol. Rapid Commun.* **2022**, 43, e2200490.
- [157] W. Peng, J. Yin, X. Zhang, Y. Shi, G. Che, Q. Zhao, J. Liu, *Adv. Funct. Mater.* **2023**, 33, 2214505.
- [158] C. Lin, Z. Huang, Q. Wang, W. Wang, W. Wang, Z. Wang, L. Liu, Y. Liu, J. Leng, *Research* **2022**, 2022, 9825656.
- [159] Y. Zhu, K. Deng, J. Zhou, C. Lai, Z. Ma, H. Zhang, J. Pan, L. Shen, M. D. Bucknor, E. Ozhinsky, S. Kim, G. Chen, S.-H. Ye, Y. Zhang, D. Liu, C. Gao, Y. Xu, H. Wang, W. R. Wagner, *Nat. Commun.* **2024**, 15, 1123.
- [160] W. Wang, Z. Luan, Z. Shu, K. Xu, T. Wang, S. Liu, X. Wu, H. Liu, S. Ye, R. Dan, X. Zhao, S. Yang, M. Xing, C. Fan, *Adv. Sci.* **2023**, 10, 2303779.
- [161] K. Lee, W. Choi, S. Y. Kim, E. B. Lee, W. T. Oh, J. Park, C. H. Lee, J. S. Lee, H. W. Bae, D. S. Jang, K. S. Lee, S. W. Yi, M. L. Kang, C. Y. Kim, H. J. Sung, *Adv. Funct. Mater.* **2023**, 33, 2300264.
- [162] J. Delaey, P. Dubruel, S. Van Vlierberghe, *Adv. Funct. Mater.* **2020**, 30, 1909047.
- [163] Z. Fang, Y. Kuang, P. Zhou, S. Ming, P. Zhu, Y. Liu, H. Ning, G. Chen, *ACS Appl. Mater. Interfaces* **2017**, 9, 5495.
- [164] A. Melocchi, M. Uboldi, N. Inverardi, F. Briatico-Vangosa, F. Baldi, S. Pandini, G. Scalet, F. Auricchio, M. Cera, A. Foppoli, A. Maroni, L. Zema, A. Gazzaniga, *Int. J. Pharm.* **2019**, 571, 118700.
- [165] M. Uboldi, C. Pasini, S. Pandini, F. Baldi, F. Briatico-Vangosa, N. Inverardi, A. Maroni, S. Moutaharrik, A. Melocchi, A. Gazzaniga, L. Zema, *Pharmaceutics* **2022**, 14, 2814.
- [166] M. Bil, E. Kijenska-Gawronska, E. Glodkowska-Mrowka, A. Manda-Handzlik, P. Mrowka, *Mater. Sci. Eng. C* **2020**, 110, 110675.
- [167] M. Bil, P. Mrówka, D. Kołbuk, W. Świążkowski, *Compos. Sci. Technol.* **2021**, 201, 108481.
- [168] N. Inverardi, G. Scalet, A. Melocchi, M. Uboldi, A. Maroni, L. Zema, A. Gazzaniga, F. Auricchio, F. Briatico-Vangosa, F. Baldi, S. Pandini, *J. Mech. Behav. Biomed. Mater.* **2021**, 124, 104814.
- [169] W. Zhou, X. Yu, Z. Zhang, X. Zou, H. Song, W. Zheng, *Int. J. Pharm.* **2024**, 650, 123670.
- [170] O. King, M. M. Pérez-Madrigal, E. R. Murphy, A. A. R. Hmayed, A. P. Dove, A. C. Weems, *Biomacromolecules* **2023**, 24, 4680.



Chengjun Zeng is currently employed at the Harbin Institute of Technology (HIT), China. He received his Ph.D. from the School of Astronautics at Harbin Institute of Technology. His research interests are concentrated on shape-memory polymer composites and 4D-printed intelligent structures.



Wei Zhao obtained his Ph.D. in mechanics from the Harbin Institute of Technology (HIT), China. His research interests are focused on smart materials and structures, metamaterial structures, energy harvesting, implantable medical devices, and so on.



Yanju Liu is a professor in the Department of Aerospace Science and Mechanics at the Harbin Institute of Technology (HIT), China. From 1999 to 2003, she served as a research fellow at Nanyang Technological University and Newcastle University. Her research encompasses smart materials and structures, including electrorheological and magnetorheological fluids, electroactive polymers, and shape-memory polymers and their nanocomposites. She has authored or coauthored over 200 scholarly publications in various scientific journals.